A STUDY ON THE MINIMUM WEIGHT DESIGN OF WING STRUCTURES SATISFYING STRENGTH, STABILITY AND FREQUENCY REQUIREMENTS

By

VALISETTY RAMAKRISHNA RAO

DEPARTMENT OF AERONAUTICAL ENGINEERING

INDIAN INSTITUTE OF TECHNOLOGY KANPUR

JULY, 1976

A STUDY ON THE MINIMUM WEIGHT DESIGN OF WING STRUCTURES SATISFYING STRENGTH, STABILITY AND FREQUENCY REQUIREMENTS

A Thesis Submitted
In Partial Fulfilment of the Requirements
for the Degree of
MASTER OF TECHNOLOGY

By
VALISETTY RAMAKRISHNA RAO

to the

DEPARTMENT OF AERONAUTICAL ENGINEERING
INDIAN INSTITUTE OF TECHNOLOGY KANPUR
JULY, 1976

Dedicated

To My Parents

CERTIFICATE

This is to certify that the thesis entitled 'A Study on the Minimum Weight Design of Wing Structures Satisfying Strength, Stability and Frequency Requirements' by Valisetty Ramakrishna Rao is a record of work carried out under our supervision and that it has not been submitted elsewhere for a degree.

S. S. Rao
Assistant Professor
Department of Mechanical Engineering
Indian Institute of Technology
KANPUR

N.G.R. Iyengar
Assistant Professor
Department of Aeronautical Engineering
Indian Institute of Technology
KANPUR

ACKNOWLEDGEMENTS

The author wishes to express his appreciation and gratitude to:

His advisor Dr. N.G.R. Iyengar, whose continuous encouragement, guidance and enthusiasm were vital to the success of this effort,

Dr. S.S. Rao, for his valuable suggestions during the course of this work,

Dr. P.N. Murthy, for introducing him to the field of Structural Optimization,

The Directorate of Aeronautics (R & D), the Ministry of Defence, the Government of India, for sponsoring this work and for providing financial assistance under the grant No. 5/ME/9.

The author also wishes to express his thanks to:

his friends, who rendered his stay at IIT/K, pleasant,

Mr. Tiwari, for his excellent typing.

ABSTRACT

In this investigation minimum weight design of general wing structures satisfying strength, stability and frequency requirements is attempted. A computer programme package is developed for the automated minimum weight design of a symmetric wing structure satisfying the strength, stability, frequency and flutter requirements. Attempts are made to reduce the number of design variables, which in turn reduce the required computational effort, by the help of a parametric study. This study indicates that uniform mass distribution can be considered for the spars and ribs without any appreciable change in the behaviour constraints. A typical wing structure is optimized satisfying the above requirements. The feasibility of employing linearly-approximated ~~redesigns~~ reanalysses is investigated. Off-design charts are obtained by a parametric study about the final optimum design point. Further improvements that can be incorporated in this study are also suggested.

CONTENTS

LIST OF IMPORTANT SYMBOLS

a	length of a rectangular plate
$\vec{a}$	vector of interpolation functions
a_∞	free stream speed of sound
A_j	Area of jth plate element
A_{123}	Area of triangle 123
$[A^i], [B^i], [C^i], [D^i]$	Component matrices used in defining the aerodynamic matrix $[Q^i]$ for ith element
$[A], [B], [C], [D]$	Component matrices used in defining the aerodynamic matrix $[Q]$
b	width of a rectangular plate
b_r	some reference length
b_s	spacing of stiffners
b_w	depth of stiffners
D_1, D_2	flexural rigidities of an orthotropic plate
D_3	torsional rigidity of an orthortropic plate
E	Youngs Modulus
$f(\vec{X})$	objective function, the weight of the wing structure in lbs.
$g_j(\vec{X})$	jth constraint
G	shear modulus
$[H_i]$	symmetric positive definite matrix in variable metric method
i	$\sqrt{-1}$, also used as an integer
$[I]$	identify matrix

$[k_r]$ reduced frequency

$[k]$ elemental stiffness matrix

$[K]$ master stiffness matrix

$[\bar{K}]$ stiffness matrix after employing plate flexural assumptions

$[K_r]$ reduced stiffness matrix for dynamic analysis

$[K_{11}]$, $[K_{12}]$, $[K_{21}]$, $[K_{22}]$ partioned components of $[K]$

ℓ_j length of jth pin-jointed bar

m number of constraints

$[m]$ elemental mass matrix

$[M]$ master mass matrix

$[\bar{M}]$ mass matrix after employing plate flexural assumptions

$[M_r]$ reduced mass matrix for dynamic analysis

M_F flutter Mach number

M_∞ free stream Mach number

N, n number of design variables

B_b number of pin-jointed bar elements

N_p number of plate elements

N_X compressive force applied to a plate

$\vec{P}$ Load vector

P_i ith generalized force

$[Q]$ airforce matrix used in flutter analysis

$[Q^i]$ airforce matrix for ith planform element

$[Q_r]$ assumbled aerodynamic matrix

r number of degrees of freedom in eigen problem

r_K penalty parameter

s	number of generalized coordinates used in flutter analysis
$\vec{S}_i$	ith direction vector
t	thickness of a plate element
t	time parameter
t_s	thickness of cover skin
$\bar{t}_s$	effective thickness of a stiffned plate
t_w	thickness of stiffners
T	kinetic energy of a structure
u,v,w	displacement components in x,y,z directions
$\vec{U}$	vector of nodal displacements
$[U]$	modal matrix
V	potential energy of a structure
$\bar{V}$	volume
V_∞	free stream velocity
V_a	Virtual work
V_F	flutter velocity
$\bar{w}$	virtual displacement
W	external work done by external applied forces
$\vec{W}$	nodal vector of w displacements
x,y,z	local coordinate system
$\bar{x},\bar{y},\bar{z}$	global coordinate system
$\vec{X}$	design vector
$\vec{Y}$	displacement vector,eigenvector
$2z(x,y)$	thickness distribution of a wing

γ	ratio of specific heats
θ	angle between search direction and gradient vector
δ	displacement (in inches)
Δp	differential pressure
Δx_k	small increment in design variable x_k
ϕ	Fiacco-McCormick penalty function
$\nabla\phi$	gradient of ϕ-function
$\vec{\sigma}$	stress vector
σ	induced stress (in psi)
σ_b	induced compressive stress in stiffned plate which causes buckling
ω	oscillation frequency
ω_F	flutter frequency
ω_i	ith natural frequency (c.p.s)
$\lambda_i = \omega_i^2$	ith eigenvalue
$[\lambda]$	coordinate transformation matrix
τ	step length in optimization
τ^*	minimizing step length
ρ_j	density of jth finite element
ρ_∞	density of air
ν	Poissons ratio
ε	a small number
$\vec{\varepsilon}$	strain vector
ξ_i	ith generalized coordinates

Superscripts

e	elemental
ℓ	lower bound
u	upper bound

Subscripts

1,2,3	denotes the quantities corresponding to nodes 1,2,3,
i,j	i,j th element
root	element at root section
tip	element at tip section

LIST OF TABLES

LIST OF FIGURES

CHAPTER 1

INTRODUCTION

During the design stages of an aircraft, it is customary to base the structural design primarily upon the requirements of strength and stiffness. The dynamic and flutter requirements are then satisfied by making modifications to the strength design by a process of trial and error. This procedure is adopted mainly because of the lack of a suitable design procedure that can handle all the requirements simultaneously and also the design modifications to satisfy the flutter requirements are not extensive for subsonic aircraft. However, in the design of large, high performance aircraft dynamic and aeroelastic requirements play nearly as prominent a role as the strength. Cases can be cited when the required margins on flutter speed could be met only through the addition of several thousand pounds of material to a wing which had already met static loading design conditions. Also it is a known fact that the aerodynamic parameters like sweepback angle, aspect ratio and thickness to chord ratio influence the dynamic and aeroelastic performance. Hence these parameters can also be included when the design modifications are made to meet the dynamic and aeroelastic requirements, as long as the resulting changes in the aerodynamic parameters does not appreciably change the aerodynamic performance.

Although techniques for the analytical prediction of dynamic and aeroelastic properties of a given structure are highly developed, the introduction of such features into formal structural procedures has not been given much consideration untill recently.

1.1 Review of Literature

During the last few years, several structural optimization investigations have been reported that deal mainly with one particularly troublesome behaviour constraint. Turner[1] developed a procedure for determining relative proportions of selected elements of an aircraft structure to attain a specified flutter speed with minimum total mass. Lagrange multipliers were employed to introduce the constraints and the resulting system of nonlinear equations was solved by the Newton-Raphson method to determine the masses of the elements of the system. The optimization of one dimensional structures like beams under aeroelastic constraints was reported by Ashley et al.[2] In this work, the authors found the solution by reducing the original problem to a set of first order differential equations by the application of Euler-Lagrange equations and the transversality conditions. Haftka[3] replaced a continuous flutter constraint by the minimum value of the constraint over the range of values of the parameters, thus reducing the computational effort. Approximate expressions are derived for the minimum value of the parametric flutter constraint.

Fox and Kapoor[4] reported a capability for minimum weight optimum design of planar truss-frame structures with distributed and concentrated mass. Inequality constraints were placed on the maximum dynamic displacements and stresses and natural frequencies of the structure were excluded from certain bands. A direct optimization method (the method of feasible directions) which consists of a design-analysis cycle was used to solve the optimization problem. McCart, et al.[5] developed a steepest-descent boundary value method for the design of structures with constraints on strength and natural frequencies. A computational algorithm was developed which implemented the steepest descent method. Sippel and Warner[6] investigated the optimization problem of simple 2 to 3 element structures of sandwich type with frequency constraints. They considered the axial vibration, flexural vibration and the rotational inertia effects of tip masses in detail. The minimum weight design of structures with a specified natural frequency requirement was considered by Turner[7], Zarghamee[8] and Rubin[9].

Kicher[10] reported a capability for finding the minimum weight design of integrally stiffened cylindrical shells by considering gross buckling, panel buckling, and skin and rib buckling as behaviour constraints. Zarghamee[11] used a combination of the Rosen gradient projection method and steepest-descent, alternate steps method of Schmit in the minimum weight design of a discretized structure with

a general stability constraint. Simites and Unghbhakorn[12], by judicious choice of the objective function and proper grouping of the design parameters accomplished the minimum weight design of stiffened cylinders under axial compression in two phases. The first optimization phases yields design charts, which are then used in the design phase to arrive at the minimum weight.

Recently there have been some attempts to include both strength and aeroelastic requirements in the optimum structural design problems. Schmit and Thornton[13] considered a highly idealized double wedge airfoil with the total propulsive work as the objective for minimization. The root angle of attack, tip deflection, root stresses and bending-torsion flutter Mach number were considered as behaviour constraints with airfoil thickness and chord length as the two design variables. An automated preliminary design procedure for simplified wing structures has been reported by Stroud, et al[14]. By idealizing the wing as an isopropic sandwich plate with a variable thickness distribution, the authors used an interior penalty function method to find the minimum weight cover thickness distribution. Strength, stability and flutter constraints were used. Giles[15] developed a procedure to include the interaction of external shape, aerodynamic loads, structural geometry and fuel mass in the fully stressed design of thin aerodynamic surfaces. Rao[16] considered strength, stability, frequency

and flutter constraints under different flight conditions (varying fuel weight). His design parameters include the thickness of covers, webs and ribs, and flange areas.

To improve upon the computational effort and expedite convergence number of investigators have suggested various refinements to the standard algorithms and different formulations of the basic optimization problems. Optimum structural design studies can, with few exceptions, be placed into three broad categories. In the first method the stated problem is attempted directly by calculus of variations. Although this approach is one of formal power and elegence it has been successful primarily with plates and portal frames[17]. This method has been applied with limited success to standard structural systems optimization because of the great analytical complexity. Studies in the second category are based on Shanley's[18] structural index approach. This procedure has been applied successfully to a variety of minimum weight design problems with strength and buckling constraints. This method has not been explored in the case of statically indeterminate structures. In the third and the most general category optimization of structural systems is examined on numerical basis using the tools of linear, non-linear and dynamic programming. This approach pioneered by Schmit[19] has dealt successfully with a wide range of structural optimization problems and has been largely responsible for the increasing involvement of optimum structural design in traditional design methods. Although this method is quite successful with a wide range of design

problems perticular attention must be given to keep down the computational effort and reduce the numerical inaccuracies due to instability while dealing with large structural systems (50 or more design variables).

Picket, Jr. et al.[20] developed a procedure to reduce the number of design variables in the automated structural synthesis of large systems. A rational procedure based on the external loads and constraints on the system was developed for generating the reduced set of coordinates (depend upon the linearly independent design like fully stressed design, fully deflected design etc.). Thus the complete design problem is replaced by much simpler optimality criteria. Another technique suggested by Pope[21] to reduce the computational effort and expedite the convergence, is to cast the original mathematical problem as a sequence of linear programming problems.

1.2 Scope of the Present Work

As stated above most of the literature is concerned with the optimization of either highly idealized structures, or with structures that deal primarily with one type of behaviour constraint, or different formulations of the basic optimization problem to expedite the convergence. Very few investigators considered all the behaviour constraints simultaneously.

In the present investigation, the feasibility of including multiple behaviour constraints in the optimum design of a symmetric wing structure, with design variables including the sweepback angle, aspect ratio and thickness to chord ratio apart from usual gauge parameters is demonstrated. Also the mass distribution of the wing is assumed to decrease linearly towards the tip of the wing. The inclusion of this feature alone may not accomplish a fully-stressed design, but nevertheless helps in that direction and also some saving in the weight can be envisaged over a uniform mass distribution. The gauge parameters, like cover thicknesses and flange areas are assumed to vary linearly along the span of the wing. A parametric study of the behaviour quantities (maximum deflection, stresses induced etc.) is conducted to study, how they are influenced by the design variables, before the actual optimization problem is taken up. This study suggested that the mass distribution of the span and ribs can be taken as uniform throughout the wing, reducing the number of gauge parameter variables to 6 in the subsequent optimization problem. After the optimum is found, off-design charts are made by conducting another parametric study. These charts help to assess the penalty in the minimum weight whenever the optimum design is slightly perturbed.

A requirement of this nature demands a number of capabilities to be assembled. First the structure has to be represented by a suitable model to determine the necessary static, dynamic and aeroelastic

characteristics. This structural idealization must be accurate enough and must be suitable for the embedment into the iterative design analysis loop of the optimization procedure. Finally for the solution of the mathematical programming problem, the partial derivatives of the behaviour constraints with respect to the design variables have to be determined.

In the present work, the finite element method, with 3 different kinds of elements, is used to model the multiweb wing structure. The constant stress triangle membrane elements and the rectangular shear panels are used to idealize the skin and web respectively. The stringers are represented as axial force members. Elastic buckling constraints are introduced by treating a typical portion of the wing skin as an isentropic stiffened plate. The second order piston theory is used in finding the flutter Mach number of the structure.

The constrained optimization problem is cast as a nonlinear mathematical programming problem. The design variables include the sweepback angle, aspect ratio, thickness to Chord ratio, cross sectional areas of the pin-jointed bar elements, thicknesses of spans,ribs, and the two linear constants which represent the skin thicknesses. The interior penalty function method, with a variable metric unconstrained minimization technique, is used in the minimum weight design problem. The minimizing step lengths are determined using cubic interpotation technique. Partial derivatives are computed using finite difference formula.

The thesis is organized into six chapters. The objective function and the design criteria are described in Chapter 2 and the problem of minimum weight design of wing structure is formulated as a nonlinear mathematical programming problem.

In Chapter 3 analytical idealization of the wing structure is considered. A method of including the elastic buckling constraint in the optimization problem is described. The derivation of the necessary inertia, stiffness and aerodynamic matrices for the formulation of flutter equations has also been presented in Chapter 3.

Chapter 4 deals with the optimization algorithm used in the present work. Reasons for using the penalty function formulation with a variable metric unconstrained minimization method are discussed.

The results of the present investigation are presented in Chapter 5, the conclusions drawn from the present study and the recommendations for the future investigation are presented in Chapter 6.

The derivation of element stiffness and mass matrices for the three types of elements used in the present work and the computer programme package developed in the present work are briefly described and presented in Appendices A & B respectively.

CHAPTER 2

FORMULATION OF THE OPTIMIZATION PROBLEM

When a means of predicting the behaviour of any design within a particular design concept is available, limitations on the performance and other external constraints on the design can be stated, and an acceptance criterion can be established, then it is possible to cast the design modification problem in the form of a mathematical programming problem. A mathematical programming problem is one in which a multivariate function $f(\vec{X})$, where $\vec{X}$ is a n-dimensional design vector, is to be optimized subject to given constraints $g_j(\vec{X}) \leq 0$, $j = 1,2,\ldots m$. The function $f(\vec{X})$ is called the objective function and its choice is governed by the nature of the problem.

2.1 Objective Function

The nature of the structural design problem is such that there will usually be many designs that perform the specified functional purposes adequately. The objective function in structural design optimization represents a basis for choice between alternate acceptable designs. Weight minimization is often taken as the objective of structural design optimization. This is in part due to the fact that weight is readily quantified, partly reflects material costs and its saving can be converted directly into increased payload or range. The minimum weight of the structure is, therefore, considered as the objective function.

2.2 Design Criteria

Characterization of structural design philosophy involves-identification of the kinds of failure modes to be guarded against. The design criteria to be satisfied are the following

(1) The elastic deflection at the tip of the wing must not exceed certain prescribed limits.

(2) The stresses induced at the root as well as tip of the wing should not exceed the yield stress of the material. This constraint is important since the cover thickness decreases from the root to the tip.

(3) The first few natural frequencies of the structure are to lie within certain bounds.

(4) Flutter frequency and Mach number should be away from the specified value. However, this constraint is not included in the final solution because the double eigenvalue analysis of flutter is to be performed $n+1$ times whenever the gradient of the function is computed, which is highly time consuming (IBM 7044 computer is used). However, the developed programme has the capability of including this constraint also.

2.3 Design Variables

The objective function and the design criteria being known the structural optimization problem of the wing can be cast as a mathematical programming problem once the design variables are choosen.

It is proposed to include sweepback angle, aspect ratio and thickness to chord ratio as the design variables in order to assess the feasibility of optimization in the presence of these variables and also to study the inter action of external shape and mass distribution of the wing. The individual thicknesses of the plate elements, cross sectional areas of the pin-jointed bars form the rest of the variables. Because of large number of finite elements involved, a group of elements are often specified by one design variable. One convenient means by which the m design variables of the optimization problem can be related to the individual thicknesses of of plate elements, cross-sectional areas of flanges and weights of tuning masses is through a design correlation table[22]. This design variable correlation table imposes additional linking constraints on the optimization problem which can be handled rather easily. Hence five pairs of variables, each pair (X_i and X_{i+1} of $X_i - x\ X_{i+1}$) representing the linearly decreasing (in spanwise direction) mass distribution of cover plate elements, web elements of spars and ribs, and flange elements of spars and ribs respectively, are considered. Thus to start with, there are ten variables representing the thickness of the cover plate elements, web elements of the spars and ribs and flange areas of the spars and ribs. However, these variables are further reduced to six, since the preliminary parametric study showed that the linearly decreasing mass distribution of the spars and ribs can be replaced by uniform mass distribution without

incurring any appreciable change in the behaviour constraints. Thus in the present optimization problem nine design variables (three variables representing the external shape and six variables representing the mass distribution of the wing) are considered.

2.4 Optimization Problem

Mathematically the optimization problem can be expressed as:

$$\text{Minimize} \qquad f(\vec{X}) = \sum_{j=1}^{N_p} A_j \rho_j X_j + \sum_{j=1}^{N_b} \ell_j \rho_j X_j \qquad (2.1)$$

subject to

$$\delta^u_{tip} - \delta_{tip} \geq 0$$

$$\sigma^u_{root} - \sigma_{root} \geq 0$$

$$\sigma^u_{tip} - \sigma_{tip} \geq 0 \qquad (2.2)$$

$$\sigma^u_{b.root} - \sigma_{b.root} \geq 0$$

$$\sigma^u_{b.tip} - \sigma_{b.tip} \geq 0$$

$$\omega_1^\ell \leq \omega_1 \leq \omega_1^u \quad , \quad \omega_2^\ell \leq \omega_2 \leq \omega_2^u$$

$$M_F - M_\infty \geq 0 \qquad (2.3)$$

and

$$X_j^\ell \leq X_j \leq X_j^u \quad , \; j = 1, \ldots n \qquad (2.4)$$

where, $f(\vec{X})$ represents the weight of the structure and δ, σ, σ_b, ω, M_F represent the behaviour quantities maximum deflection, maximum induced stress, buckling stress, natural frequency and

flutter Mach number. Eq. (2.4) represent the geometrical or side constraints, which impose limits on the size of the design variables, X_j. It can be seen that the objective function, Eq. (2.1) as well as the behaviour constraints Eqs. (2.2) are non-linear functions of the design variables. The constraint, Eq. (2.3) is not included when the final optimization problem is run. The solution procedure of this optimization problem is discussed in Chapter 4.

CHAPTER 3

IDEALIZATION OF WING STRUCTURE

3.1 Static Analysis

The prediction of static, dynamic and aeroelastic behaviour of a wing structure represents a problem of extreme complexity. The geometric and load conditions are non uniform. Elementary theories are often incapable of providing accurate results. Extensive efforts have been expended over the years in the development of techniques to provide results of acceptable accuracy, and this resulted in the development of finite element method as one of the most convenient ways to handle complex structures.

The finite element method of structural analysis, used in the present investigation, consists of representing wing structure as an assembly of triangular membrane cover elements (9 degrees of freedom), rectangular shear web elements (12 degrees of freedom) and pin-jointed flange elements (6 degrees of freedom) as shown in Fig. 3.1. Triangular membrane cover elements carry direct stresses. The internal members (spars & ribs) are effective in shear. The pin-jointed flange elements represent the direct stress carrying capacity of the stringers. The edge displacements are assumed linear in all the elements and shear stress constant in the web element. The available computer core (32K, IBM 7044) eliminated

the possibility of using more accurate plate bending elements (non-conforming triangular element with 18 degrees of freedom, conforming triangular element with 36 degrees of freedom) in the place of triangular membrane cover elements.

Studies made by Gallagher, et al.[23] indicated that the static behaviour of a wing structure is predominantly influenced by the choice of web element idealization, and not by the choice of cover panel idealization. Hence, a comparative study of the displacement and eigenvalue results is made to find the rates of convergence and accuracies available with different web idealizations. Before presenting the numerical results of the comparative study, the derivation of the element stiffness and mass matrices will be outlined briefly.

3.1.1 Derivation of element stiffness and mass matrices

The element stiffness and mass matrices are derived from the local assumed displacement or stress field. Let the true displacement state of any element $\vec{u}(x,y,z)$ be related to the nodal displacements $\vec{U}$ by

$$\vec{u}(x,y,z) = [a(x,y,z)]\ \vec{U} \tag{3.1}$$

If the strain-displacement relation is denoted by

$$\vec{\varepsilon}(x,y,z) = [b(x,y,z)]\ \vec{U} \tag{3.2}$$

the matrix $[b(x,y,z)]$ can be obtained by the differentiation of the matrix $[a(x,y,z)]$. The kinetic energy and potential

energy of the element are, respectively, given by

$$T^{(E)} = \frac{1}{2} \int_{\bar{V}} \rho \dot{\vec{u}}^T \dot{\vec{u}} \, d\bar{V} \tag{3.3}$$

and

$$V^{(E)} = \frac{1}{2} \int_{\bar{V}} \vec{\varepsilon}^T \vec{\sigma} \, d\bar{V} \tag{3.4}$$

where ρ is the mass density, $\bar{V}$ is the volume of the element and $\dot{\vec{u}}$ is the velocity. The stress vector is related to the strain vector $\bar{\varepsilon}$ by the Hooke's law

$$[\vec{\sigma}] = [c] \vec{\varepsilon} \tag{3.5}$$

By assuming the generalized displacements to be time dependent, the potential and kinetic energies of the element can be expressed as

$$V^{(E)} = \frac{1}{2} \dot{\vec{U}} [k] \dot{\vec{U}} \tag{3.6}$$

and

$$T^{(E)} = \frac{1}{2} \dot{\vec{U}} [m] \dot{\vec{U}} \tag{3.7}$$

where $[k]$ and $[m]$ are, respectively, the stiffness and equivalent mass matrices of the element. By substituting Eqs. (3.1), (3.2) and (3.5) into Eqs. (3.3) and (3.4), we obtain

$$V^{(E)} = \frac{1}{2} \vec{U}^T \left(\int_{\bar{V}} [b]^T [c] [b] \, d\bar{V} \right) \vec{U} \tag{3.8}$$

and

$$T^{(E)} = \frac{1}{2} \dot{\vec{U}}^T \left(\int_{\bar{V}} \rho [a]^T [a] \, d\bar{V} \right) \dot{\vec{U}} \tag{3.9}$$

By comparing Eq. (3.6) with Eq. (3.8) and Eq. (3.7) with Eq. (3.9), one obtains the stiffness and mass matrices of the finite element

$$[k] = \int_{\bar{V}} [b]^T [c] [b] \, d\bar{V} \tag{3.10}$$

$$\text{and} \qquad [m] = \int_{\bar{V}} \rho\, [a]^T [a]\, d\bar{V} \qquad (3.11)$$

The integrals in Eqs. (3.10) and (3.11) can be evaluated explicitly if the assumed displacement or stress distribution within the finite element is known. The detailed derivation of the mass and stiffness matrices is presented in Appendix A.

3.1.2. Numerical results for multiweb wing structures

Several wing structures are analyzed for static deflections and natural frequencies by using the following idealizations in order to arrive at an accurate and simpler finite element idealization for the wing.

(1) The triangular membrane elements and the rectangular membrane elements are used for the idealization of skins and webs respectively.

(2) Both the cover plates and the webs are idealized by the triangular membrane elements.

(3) The cover skins are modelled by the triangular membrane elements and the webs are idealized by the triangular shear elements.

(4) The cover plates are idealized by the triangular membrane elements and the webs are modelled with rectangular shear panels.

The pin-jointed bar elements are used to model the stringers in all the above idealizations.

The model wings shown in Fig. 3.2 were tested and analyzed for static deflection by Gallgher, et al.[23] and also by Rao[16]

The dimensions of these model wings are given in Ref. 23. The results for the static analysis and the eigenvalue analysis are presented in Tables 3.1 and 3.2 respectively. These results are found to be in complete agreement with those reported in References 23 and 16.

It is observed that the idealization (4) gives results which are close to the experimental values (Ref. 23) even with a relatively coarse mesh size in the case of static analysis. Eventhough no experimental frequencies are available for comparison, the idealization which gives lower frequency values is generally considered to be more accurate. On this basis also, the idealization (4) can be seen to be more accurate. Hence in the subsequent analysis this idealization is used.

3.1.3 Deflection and stress analysis

In the optimization problem the wing is assumed to carry a specific pay load which in turn is assumed to act as equally distributed point loads at the nodal points. In the present work, a clamped boundary condition is specified along the root of the wing thereby neglecting any influence of the flexibility of the fuselage. The number of degrees of freedom involved in the static analysis are reduced to one-half by making the plate flexural assumptions. This is made possible by assuming the wing to be symmetric about its middle plane and by choosing the

node points on the top and bottom surfaces of the wing also to be symmetric. By assuming that (a) the vertical displacements of the upper and lower surface points at a given planform location are equal, and (b) the implane displacement of these same respective points are equal and opposite, the number of the displacement variables can be reduced by one-half.

The matrix formulation (displacement method) of the general structural analysis problem results in the equation

$$[K]\vec{Y} = \vec{P} \tag{3.12}$$

where $[K]$ is the master stiffness matrix of the structure. The vectors $\vec{Y}$ and $\vec{P}$ represents respectively the displacement and the load vectors. The assembly of the master stiffness matrix from the corresponding element matrices and the solution of Eq. (3.12) follow the standard procedure of matrix structural analysis. The stresses induced in the finite elements can be determined from the known nodal displacements $\vec{Y}$ by using the stress-strain and the strain-displacement relations of the linear elasticity. Having determined the displacement and stress field. The maximum deflection of the structure and the stresses induced in the critical sections of the structure can be restricted by placing bounds upon them.

$$\begin{aligned} -\delta^{u}_{tip} + \delta_{tip} &\leq 0 \\ -\sigma^{u}_{root} + \sigma_{root} &\leq 0 \\ -\sigma^{u}_{tip} + \sigma_{tip} &\leq 0 \end{aligned} \tag{3.13}$$

3.2 Dynamic Analysis

The order of the flutter problem may be reduced by introducing the first few natural modes of the structure as generalized coordinates[16,24]. Thus the linear eigenvalue problem

$$[\bar{K}]\ \vec{Y} = \lambda [\bar{M}]\ \vec{Y} \qquad (3.14)$$

is to be solved inorder to set up the flutter equations. Moreover bounds are to be placed on the natural frequencies of the structure so that any possible resonance, that might be caused due to mild harmonic forcing, will be avoided. The eigen value analysis refers to determining the scalar quantities λ_i (eigen values) and the corresponding non trivial solutions $\vec{Y}_i$ (eigen vectors) for the given master matrices $[\bar{K}]$ & $[\bar{M}]$. Power method is used to obtain the eigen values and the associated eigen vectors.

For any given degrees of freedom the determination of eigen-values and eigen vectors is more expensive than a static solution. It is, therefore, desirable to limit the degrees of freedom of the already "discrete" system so as to make the eigen-solution economical. Hence the static condensation reduction technique suggested by Turner, et al.[25] is employed in the present work. The degrees of freedom associated with the transverse displacements are retained by eliminating those corresponding to the inplane displacements. Thus the order of the eigen problem is reduced to one-third of the corresponding statics solution.

If the load vector ($\vec{P}_2$) corresponding to the inplane degrees of freedom ($\vec{Y}_2$) is $\vec{0}$, then the expressions for the reduced stiffness and mass matrices can be given respectively as,

$$[K_r] = [K_{11}] - [K_{12}]\ [K_{22}]^{-1}\ [K_{21}] \tag{3.15}$$

and

$$[M_r] = [M_{11}] - [M_{12}]\ [K_{22}]^{-1}\ [K_{21}] - [K_{12}]\ [K_{22}]^{-1}\ [M_{21}] + [K_{12}]\ [K_{22}]^{-1}\ [M_{22}]\ [K_{22}]^{-1}\ [K_{21}] \tag{3.16}$$

In the case of the reduced stiffness matrix $[K_r]$, Eq. (3.15), none of the structural complexity is lost since all elements of the original stiffness matrix contribute. However, in the reduced mass matrix, combinations of stiffness and mass elements appear. The result is that the original eigen value problem is closely but not exactly preserved. The natural vibrations of a box beam[16] shown in Fig. 3.3 are studied in order to see the difference between the results given by the reduced eigen problem and original eigen problem. The results (presented in Table 3.3) indicate, that the first few (8) frequencies and mode shapes obtained from the reduced eigen value problem, are found to be in good agreement with those given by the original problem. This is not considered to be a serious problem since in the present work only the first three or four frequencies are considered in the flutter analysis.

3.3 Stability Analysis

A wing structure may fail in any of the failure modes of instability such as over all buckling, skin buckling and stiffener

buckling. Gross buckling of a structure can be analyzed by using the concept of geometrical stiffness[11,26]. However panel (stiffened plate enclosed between the spars & ribs) buckling is more critical compared to gross buckling of wing. Hence gross buckling of the wing is not considered in the present analysis.

In the chapter, a method[16] of including the skin and stiffener buckling failure modes in the optimum design problem is considered. Since the covers of a wing structure perform a contouring as well as a load-carrying function, the local instability modes of failure play an important role in the supersonic regime. Any change in the airfoil contour caused by local buckling might lead to an inadmissible rise in the drag at high speeds.

In the modern high performance aircraft the cover skins of the wing are usually provided with integral grid type stiffners to achieve higher buckling strength for the same solidity. For the purpose of present analysis, the portion of the grid-stiffened plate enclosed between the spars and ribs is considered to be rectangular and simply supported along the four edges. The rectangular plate is assumed to have a 0°- 90° grid configuration with longitudinal and transverse stiffners of identical shape and spacing as shown in Fig. 3.4.

3.3.1 Buckling of a stiffened plate

When the stiffener spacings for the plate are small relative to the over all length and width of the plate, it is possible to

use orthotropic plate theory to determine the buckling stress. The governing differential equation for the buckling of a simply supported flat orthotropic plate under axial compression is given by[27]

$$D_1\frac{\partial^4 w}{\partial x^4} + D_2\frac{\partial^4 w}{\partial x^4 y} + 2D_3\frac{\partial^4 w}{\partial x^2 \partial y^2} + N_X\frac{\partial^2 w}{\partial x^2} = 0 \qquad (3.17)$$

where $D_1 = \dfrac{(EI)_X}{1-\nu_X\nu_Y}$ = average flexural rigidity of a unit transverse cross-section

$D_2 = \dfrac{(EI)_Y}{1-\nu_X\nu_Y}$ = average flexural rigidity of a unit longitudinal cross section.

$$D_3 = \frac{1}{2}(\nu_X D_2 + \nu_Y D_1) + 2(GI)_{XY}$$

$2(GI)_{XY}$ = average unit torsional rigidity

ν_X, ν_Y = Poisson's ratio in the directions x and y.

w = transverse displacement

N_X = compressive force per unit length.

Assuming that plate buckles into one half sine wave and substitution of

$$w(x,y) = A \sin\frac{\pi x}{a} \sin\frac{\pi y}{b} \qquad (3.18)$$

in Eq. (3.17), one obtains

$$\sigma_{gross} = \frac{\pi^2}{b^2 t_s}\left(D_1\frac{b^2}{a^2} + D_2\frac{a^2}{b^2} + 2D_3\right) \qquad (3.19)$$

The smallest value for critical stress is obtained when

$$\frac{a}{b} = \left(\frac{D_1}{D_2}\right)^{1/4} \tag{3.20}$$

and the value is

$$\sigma_{gross} = \frac{2\pi^2}{b^2 \bar{t}_s} \left(\sqrt{D_1 D_2} + D_3 \right) \tag{3.21}$$

The flexural rigidities for the symmetric grid are given by

$$D_1 = D_2 = \frac{E}{12(1-\nu^2)} \, b_w^2 \, t_s r_b r_t \left(\frac{4 + r_b r_t}{1 + r_b r_t}\right) \tag{3.22}$$

where $E = E_X = E_Y$

$\nu = \nu_X = \nu_Y$

$r_b = b_w / b_s$

$r_t = t_w / t_s$

and b_w, b_s, t_w, t_s are the plate and stiffener dimensions as shown in Fig. 3.4.

The torsional rigidity of the stiffened plate D_3 is usually considered to be small compared to D_1 and D_2 and the effective thickness of the plate $\bar{t}_s$ is given by

$$\bar{t}_s = t_s \left(1 + r_b r_t\right)$$

The theory based on Eq. (3.17) applies to stiffening systems which are symmetrical with respect to the middle surface of the skin. The assymetry of the stiffening system causes bending to proceed simultaneously with axial loading, and thus the results of a buckling analysis for this resembles those for an initially

imperfect column. However, past studies on the buckling of an integrally stiffened plate with a one sided stiffener system[28] indicate that, although some small amount of bending is evident immediately upon the application of axial load, the maximum load carrying ability of the plate is essentially the same as the critical load obtained from Eq. (3.21).

3.3.2 Local buckling of a stiffened plate

If the skin is thin compared to the stiffeness, it is possible for the individual panel enclosed between the stiffeners to buckle as a square plate while the stiffeners undergo a stable inplane deflection. In this case, the buckling stress is given by

$$\sigma_{local} = \frac{4\pi^2 E}{12(1-\nu^2)} \frac{t_s^2}{b_s^2} \tag{3.23}$$

By considering the simultaneous occurence of the above two failure modes, Gerard[29] derived the optimum values of the geometric parameters r_b and r_t as

$$(r_b)_{optimum} = 0.425$$
$$(r_t)_{optimum} = 1.300 \tag{3.24}$$

By using these optimum values, the buckling stress of the isotropic stiffened plate can be expressed as

$$\sigma^{(u)}_{buckle} = 0.3101 \frac{E}{(1-\nu^2)} \frac{b_s^2}{b^2} \tag{3.25}$$

3.4 Flutter

Flutter is defined as a dynamic instability occuring in an aircraft in flight at a speed called the flutter speed, where the elasticity of the structure plays an essential part.

In most cases, an adequate evaluation of the flutter condition is obtained by considering an infinitesimal perturbation about the deformed equilibrium position, and analyzing vibration with exponential time dependence, since all other motions can be built up therefrom by superposition. Hence, theoretical flutter analysis usually consists of assuming in advance that all dependent variables are proportional to $e^{i\omega t}$ (ω real), and then finding combinations of M_∞ and ω for which this actually occurs[30]. This leads to a complex eigen-value problem where there are two characteristic numbers which determine flutter Mach number and frequency.

3.4.1 Formulation of flutter equations

Lagrange equations in terms of the generalized coordinates ξ_i are used to derive the flutter equations[16,31],

$$\frac{d}{dt}\left(\frac{\partial T}{\partial \dot{\xi}_i}\right) - \frac{\partial T}{\partial \xi_i} + \frac{\partial V}{\partial \xi_i} + P_i = 0, \quad i = 1,2,\ldots s \qquad (3.26)$$

where T and V are, respectively, the kinetic and potential energies, P_i is the ith generalized force, and s is the number of generalized coordinates considered in the flutter problem.

For a discretized structure, the kinetic and potential energies can be expressed as

$$T = \frac{1}{2} \dot{\vec{\xi}} [M] \dot{\vec{\xi}} \tag{3.27}$$

$$V = \frac{1}{2} \vec{\xi} [K] \vec{\xi} \tag{3.28}$$

and the generalized force vector is given by

$$\vec{P} = [Q] \vec{\xi} \tag{3.29}$$

where $[Q]$ is the aerodynamic matrix.

By substituting Eqs. (3.27) to (3.29) into Eq. (3.26), one obtains the equations for steady-state oscillations of the system in a state of neutral stability as

$$[-\omega^2 [M] + [K] + [Q]] \vec{\xi} = \vec{0} \tag{3.30}$$

where a harmonic time dependence, with a circular frequency is assumed for the variables ξ_i.

(

Derivation of Mass matrix

For a continuous plate-like structure, the kinetic energy is given by

$$T = \frac{1}{2} \iint t \rho \left(\frac{\partial w}{\partial t}\right)^2 dx\, dy \tag{3.31}$$

where

$t(x,y)$ is the thickness distribution,

$\rho(x,y)$ is the mass density per unit area, and

$w(x,y,t)$ is the displacement at any point.

For a discretized structure

$$w(x,y,t) = \vec{W}^T \vec{a} \tag{3.32}$$

where

$\vec{W}$ is a column vector of nodal displacements corresponding to the variable w, and

$\vec{a}$ is a column vector of interpotation functions in x and y.

Further, if the deflection pattern can be described by the superposition of the first 's' natural modes

$$\vec{W}(t) = [\overset{i}{U}] \vec{\xi}(t) \tag{3.33}$$

where

$[U^i]$ is the element modal matrix pertaining to the displacement w(for i^{th} element), and

$\vec{\xi}$ is the vector of modal participation coefficients.

One obtains

$$w(x,y,t) = \vec{\xi}^T [U^i]^T \vec{a} \tag{3.34}$$

Thus the kinetic energy of the i^{th} element can be expressed as

$$T^i = \frac{1}{2} \iint \rho t \dot{w} \dot{w} \, dxdy \tag{3.35}$$

where dot indicates differentiation with respect to time.

Substituting Eq. (3.34) into Eq. (3.35) we obtain

$$T^i = \frac{1}{2} \dot{\vec{\xi}}^T [U^i]^T [m^i] [U^i] \dot{\vec{\xi}} \tag{3.36}$$

where

$$[m^i] = \iint \rho t \vec{a} \vec{a}^T \, dxdy = \text{discretized mass of the } i^{th} \text{ element} \tag{3.37}$$

The kinetic energy of the assembled structure associated with all elements can be expressed as

$$T = \frac{1}{2} \dot{\vec{\xi}}^T [\bar{U}]^T [\bar{M}] [\bar{U}] \dot{\vec{\xi}} \tag{3.38}$$

where $[\bar{M}]$ is the $r \times r$ total mass matrix of the structure, and $[\bar{U}]$ is the $r \times s$ modal matrix, in which the jth column represents the jth normal mode of the structure.

If all the nodal degrees of freedom r are used in the eigenvalue analysis, the mass matrix $[M]$ of Eq. (3.30) is given by

$$\underset{s\times s}{[M]} = \underset{s\times r}{[\bar{U}]^T} \underset{r\times r}{[\bar{M}]} \underset{r\times s}{[\bar{U}]}$$

Derivation of stiffness matrix

The potential energy of a continuous plate-like structure is given by

$$V = \frac{1}{2} \iint K_1(x,y)\, w^2(x,y,t)\, dxdy \tag{3.40}$$

where K_1 is the stiffness influence coefficient at any point.

The potential energy of the i^{th} element can be expressed similar to Eq. (3.36) as

$$V^i = \frac{1}{2} \dot{\vec{\xi}}^T [U^i]^T [K^i] [U^i] \dot{\vec{\xi}} \tag{3.41}$$

where $[K^i]$ is the element stiffness matrix given by

$$[K^i] = \frac{1}{2} \iint t\, \vec{a}\, K_1\, \vec{a}^T\, dxdy \tag{3.42}$$

The potential energy of the assembled structure by considering

all the displacement variables is given by

$$V = \frac{1}{2} \vec{\xi}^T [\bar{U}]^T [\bar{K}] [\bar{U}] \vec{\xi} \qquad (3.43)$$

Hence the stiffness matrix of Eq. (3.30) is given by

$$[K] = [\bar{U}]^T [\bar{K}] [\bar{U}] \qquad (3.44)$$

Derivation of Aerodynamic matrix

Second order piston theory[32] is used in deriving the aerodynamic forces acting on the wing. The basic assumption of this theory is that the pressure at any point on the wing depends only on the normal component of fluid velocity at that point, and is related to the later in the same manner as the pressure behind a piston moving in a one-dimensional cylinder. Obviously, 3-dimensional effects are not included in this theory. However these effects on thin wings are relatively small at high flight speeds.

According to this theory, the pressure differential is given by (with the factor $e^{i\omega t}$ suppressed)

$$\Delta_p(x,y) = 2 \rho_\infty a_\infty \left(1 + \frac{\gamma+1}{2} \frac{v_\infty}{a_\infty} \frac{\partial Z}{\partial x}\right) \left(v_\infty \frac{\partial w}{\partial x} + i\omega w\right) \qquad (3.45)$$

where

ρ_∞ = mass density of air

a_∞ = speed of sound

γ = ratio of specific heats = 1.4

v_∞ = free stream velocity

$2Z(x,y)$ = thickness distribution of wing as shown in Fig. 3.5

The aerodynamic matrix of a plan form element can be derived through a calculation of virtual work. The virtual work for the i^{th} element is given by

$$V_a = \iint \bar{w}\, \Delta p \; dxdy$$

$$= 2\,\rho_\infty a_\infty v_\omega \iint \bar{w}\, \frac{\partial w}{\partial x}\, dxdy + \rho_\infty(\gamma+1)v_\infty^2 \iint \bar{w}\, \frac{\partial z}{\partial x}\, \frac{\partial w}{\partial x}\, dxdy$$

$$+ i\,2\,\rho_\infty a_\infty \omega \iint \bar{w}\, w\, dxdy + i\,\rho_\infty(\gamma+1)\, v_\infty \omega \iint \bar{w}\, \frac{\partial z}{\partial x}\, w\, dxdy \qquad (3.46)$$

where $\bar{w}$ is the virtual displacement and the integration is over the area of the element.

Introducing Eq. (3.32) into (3.46) yields

$$V_a = \vec{\bar{w}}^T [Q^i]\, \vec{w}$$

where the required aerodynamic matrix (whose order is equal to the number of nodes of the ith element) $[Q^i]$ is given by

$$[Q^i] = 2\,\rho_\infty a_\infty\, v_\infty\, [A^i] + 2i\,\rho_\infty a_\infty\, \omega\, [B^i] +$$

$$\rho_\infty\,(\gamma+1)\, v_\infty^2\, [C^i] + i\,\rho_\infty(\gamma+1)\, v_\infty\, \omega\, [D^i] \qquad (3.47)$$

with

$$[A^i] = \iint \vec{a}^T\, \frac{\partial \vec{a}}{\partial x}\, dxdy$$

$$[B^i] = \iint \vec{a}^T \vec{a}\, dxdy \qquad (3.48)$$

$$[C^i] = \iint \frac{\partial z}{\partial x}\, \vec{a}^T\, \frac{\partial \vec{a}}{\partial x}\, dxdy$$

$$[D^i] = \iint \frac{\partial z}{\partial x}\, \vec{a}^T \vec{a}\, dxdy$$

In the present work, down stream slope of an element is taken as the average slope of its nodes. Also triangular membrane elements represent the planform elements and the vector of interpotation functions for these elements is given by

$$\vec{a}\,(x,y) = \frac{1}{2A_{123}} \begin{Bmatrix} (y_3 - y_2)\,(x - x_2) - (x_3 - x_2)\,(y - y_2) \\ (y_1 - y_3)\,(x - x_3) - (x_1 - x_3)\,(y - y_3) \\ (y_2 - y_1)\,(x - x_1) - (x_2 - x_1)\,(y - y_1) \end{Bmatrix} \quad (3.49)$$

where A_{123} is the area of the element shown in Fig. (3.6). The double integrals of Eqs. (3.48) are evaluated using the following integration formulae.

If the origin is at the centroid of the triangle, then over the area of the triangle

$$\begin{aligned} \int\int dxdy &= A_{123} \\ \int\int xdxdy &= 0 \\ \int\int ydxdy &= 0 \\ \int\int x^2dxdy &= \frac{A_{123}}{12}(x_1^2 + x_2^2 + x_3^2) \\ \int\int y^2dxdy &= \frac{A_{123}}{12}(y_1^2 + y_2^2 + y_3^2) \\ \int\int xydxdy &= \frac{A_{123}}{12}(x_1y_1 + x_2y_2 + x_3y_3) \end{aligned} \quad (3.50)$$

Since only a translation of X, Y axes is involved, the transformation matrix is simply an identity matrix.

The aerodynamic matrix for the assembled structure is obtained from an assemblage of the individual plan form element matrices $[\,Q^{i}\,]$ by the standard procedures of structural analysis. Thus the airforce matrix to be used in Eq. (3.30) can be obtained as

$$[Q] = 2\,\rho_\infty a_\infty \sqrt{\Delta}\,[A] + 2\,i\,\rho_\infty\, a_\infty\, \omega\,[B] + \rho_\infty\,(\gamma+1)\,v_\infty^2\,[C] + i\,\rho_\infty(\gamma+1)\,v_\infty\,\omega[D] \qquad (2.51)$$

where $[A] = [U]^T\,[A_r]\,[U]$ (3.52)

$$[D] = [U]^T\,[D_r]\,[U]$$

3.4.2. Solution of the flutter problem

The requirement for non trivial solution to Eq. (3.30) is that the determinent of the coefficient matrix of $\vec{\xi}$ must vanish. Thus the flutter equation becomes

$$|\,[K] - w^2\,[M] + [Q]\,| = 0 \qquad (3.53)$$

The Eq. (3.53) represents a complex, nonlinear, double eigenvalue problem since there are two unknowns, free stream velocity v_∞ and oscillation frequency ω. Eq. (3.53) can be written in a more convenient form by noting that

$$[M] = [\,M_{ii}\,] \qquad (3.54)$$

and $$[K] = [\,w_i^2\,M_{ii}\,]$$

when the normal modes of vibration are used as generalized coordinates. Substituting Eqs. (3.54) into Eq. (3.53) and with

some rearrangement, one obtains

$$\left| \frac{V}{a_\infty} \frac{1}{2\rho_\infty} \left[M_{ii} \left\{ X \left(\frac{\omega_i}{\omega_1}\right)^2 - 1 \right\} \right] + \left(\frac{b_r}{k_r}\right)^2 \left([A] + \frac{\gamma+1}{2} \frac{V}{a_\infty} [C] \right) \right.$$

$$\left. + i \left(\frac{b_r}{k_r}\right) \left([B] + \frac{\gamma+1}{2} \frac{V}{a_\infty} [D] \right) \right| = 0 \qquad (3.55)$$

with $X = \left(\frac{\omega_1}{\omega}\right)^2$,

$k_r = (b_r \frac{\omega}{V})$ = reduced frequency, and

b_r = some reference length.

The Eq. (3.55) with Mach number $(\frac{V}{a_\infty})$ and reduced frequency (k_r) as the unknowns is solved by V-g method[30], a double iterative process.

3.4.3 Numerical example.

In order to test the accuracy of the flutter equations and the flutter analysis program, a double wedge airfoil shown in Fig. (3.7) is analyzed for flutter. The supersonic flutter analysis of this airfoil was previously reported by Schmit and Thornton[13]. In this work authors assumed a beam-type structural behaviour in determining the bending-torsion flutter characteristics of the wing.

In the work reported by Rao[16], the same problem is analyzed by some finite element formulation, with 40 triangular membrane elements as shown in Fig. (3.6), 55 degrees of freedom in eigen-value analysis and 4 degrees of freedom in flutter analysis. In the present work the same problem is analysed with 15 degrees of

freedom in eigenvalue analysis and 3 degrees of freedom in flutter analysis. The results are reported in Table 3.4. The present analysis underestimates the flutter Mach number by about 5%. This can be considered as good agreement since the degrees of freedom in present flutter analysis are only 3.

TABLE 3.1

DISPLACEMENT RESULTS FOR MULTIWEB WING STRUCTURES

Uniform total load applied = 1500 lb.

Type of wing structure	Maximum tip deflection in inches				
	idealization(1)	idealization(2)	idealization(3)	idealization(4)	Experimental (Ref. 23)
Model 3 (sweepback 45°)	0.445	0.240	0.280	0.704	0.797
Model 5 (sweepback 30°)	0.613	0.303	0.316	1.345	2.120

TABLE 3.2

EIGENVALUE RESULTS FOR MULTIWEB WING STRUCTURES

Type of wing structure	First natural frequency (rad./sec.)			Second natural frequency (rad./sec.)		
	idealization (1)	idealization (3)	idealization (4)	idealization (1)	idealization (3)	idealization (4)
Model 3 (sweepback 45°)	578	725	468	1482	1594	1392
Model 5 (sweepback 30°)	606	846	416	1522	1676	1402

TABLE 3.3

NATURAL FREQUENCIES OF THE BOX BEAM

Number of the Eigenvalue	Natural frequency (rad./sec.)		mode shape
	60 degrees of freedom	20 degrees of freedom	
1	43.0	43.8	first bending mode
2	88.5	88.7	Torsional mode
3	170.8	171.2	
4	235.5	235.8	second bending mode
5	318.9	319.1	
6	395.4	395.7	
7	455.7	456.0	
8	504.3	504.7	
9	602.5	-----	Inplane mode
10	704.1	704.2	

Table 3.4

RESULTS OF FLUTTER ANALYSIS FOR A DOUBLE WEDGE AIRFOIL

Attitude = 30,000 ft, material = steel

T = 1.50 ft, C = 7.50 ft, t_c = .038 ft

Naturel frequencies (rps)	Flutter frequency (cps)	Flutter Mach number		
		Ref.13	Ref.16	Present analysis
44.60				
201.46	22.65	11.77	13.37	14.10
217.53			-11.99	+ 5.45
			% error	% error
219.06				

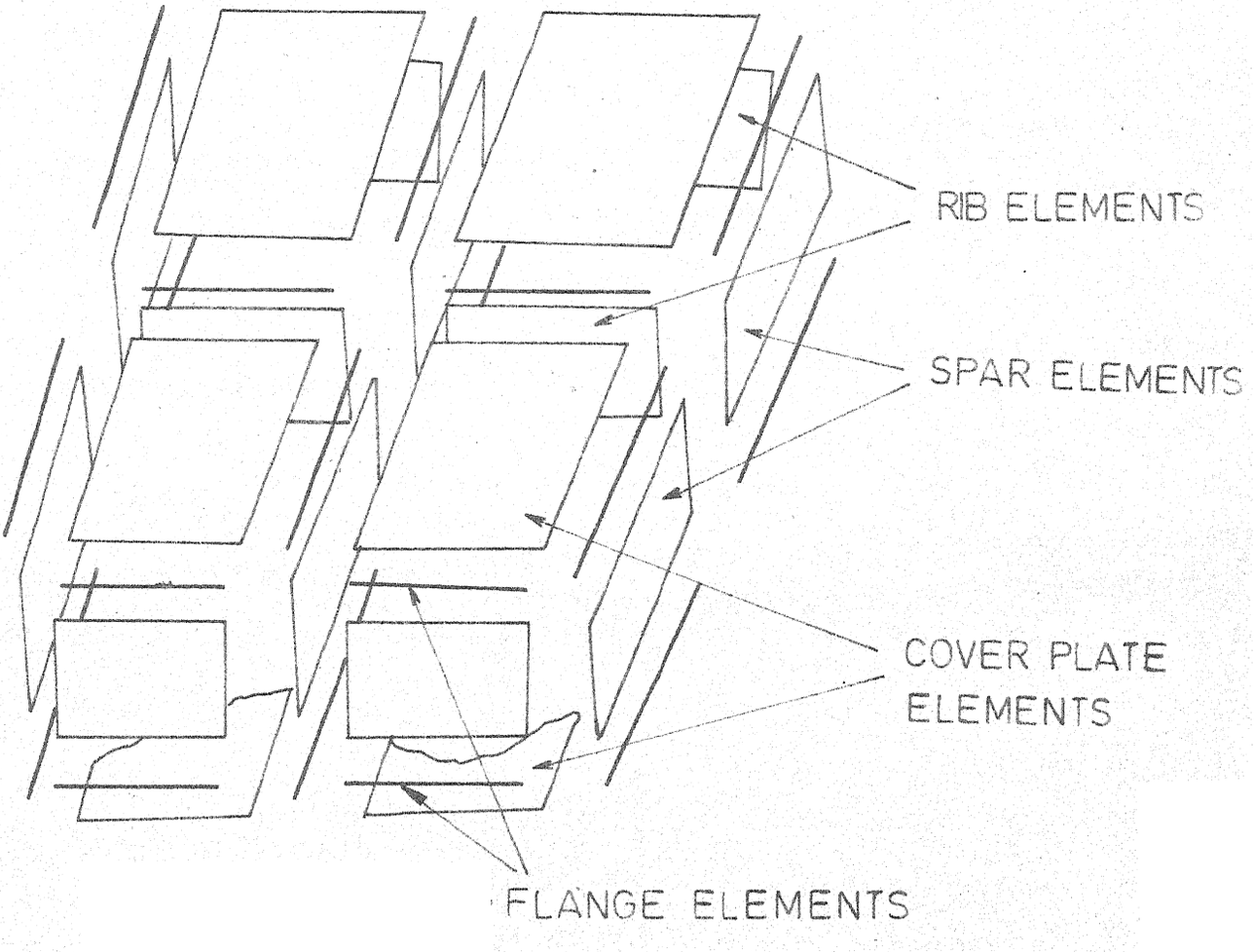

FIG. 3.1 FINITE ELEMENT IDEALIZATION FOR A SIMPLE WING STRUCTURE

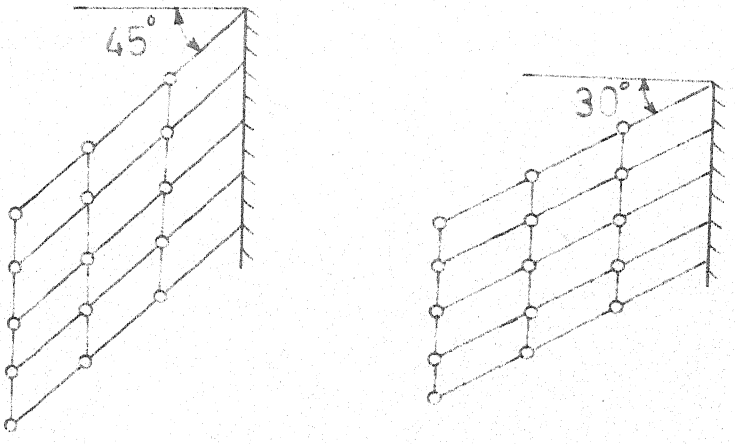

MODEL 3 MODEL 5

FIG·3·2 MULTIWEB BOX TYPE WING STRUCTURES

(Geometry and node point locations and other dimensions in reference 23)

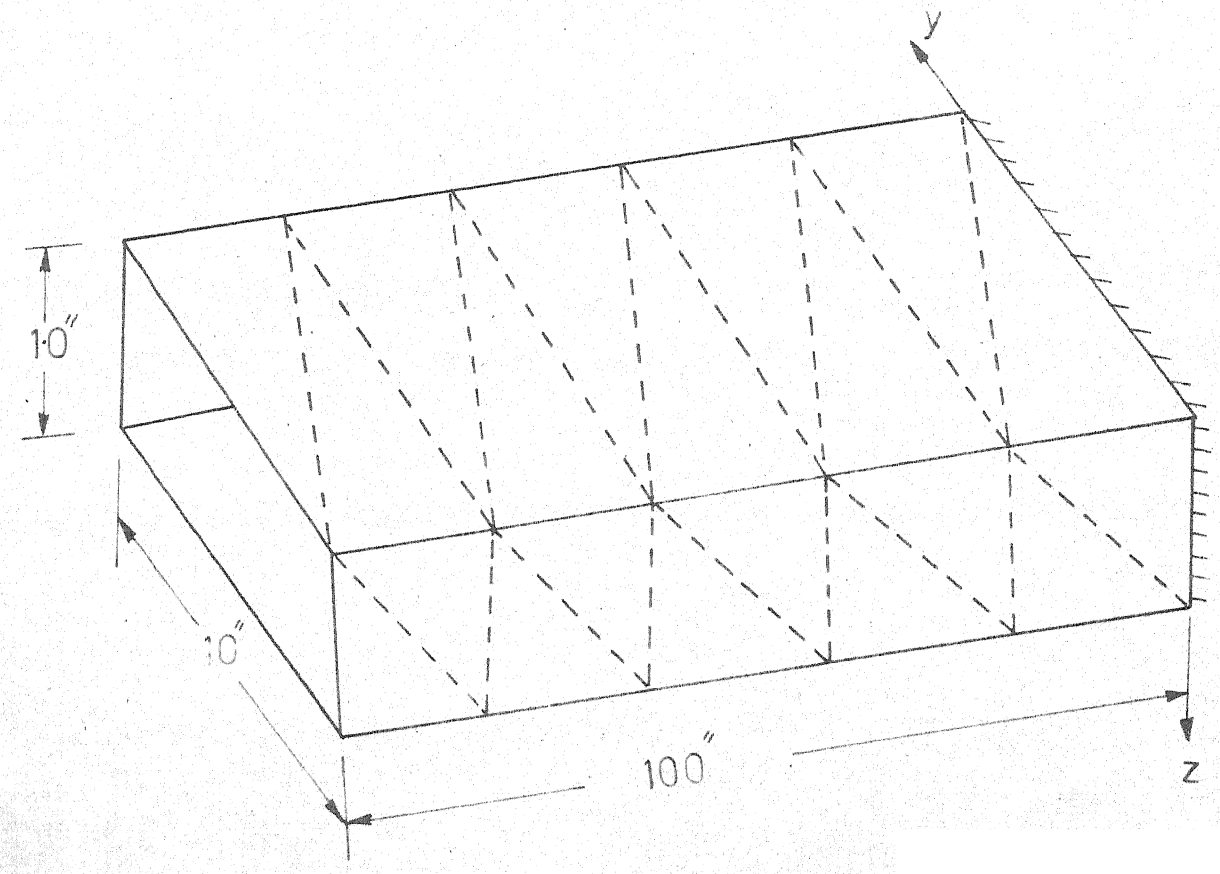

Material: steel

Cover thickness: 0·05″

Web thickness: 0·01″

Idealization: cover plates - triangular membrane elements

Webs - shear triangles

FIG. 3·3 A CANTILEVER BOX BEAM

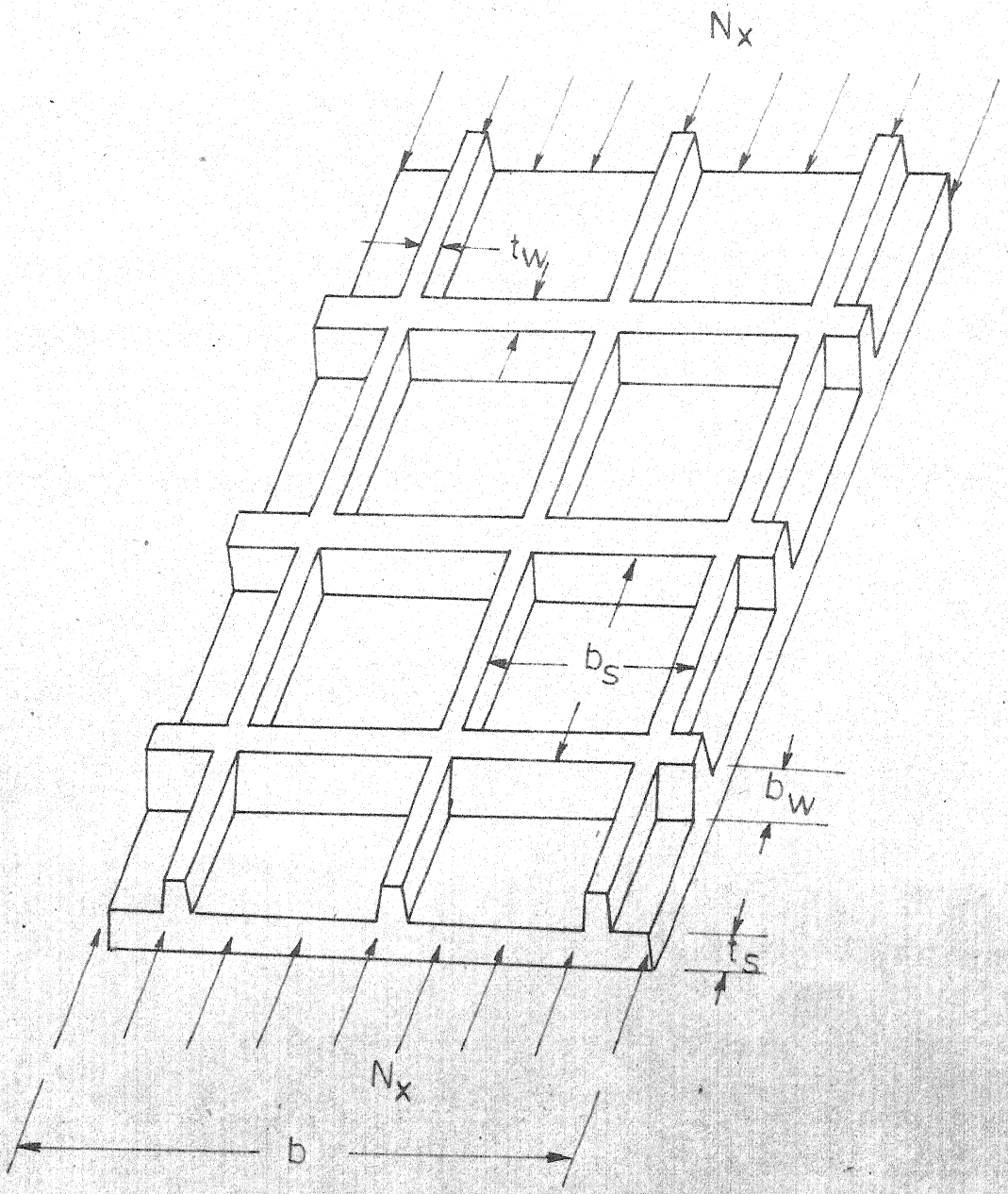

Non-dimensional parameters $r_b = \frac{b_w}{b_s}$, $r_t = \frac{t_w}{t_s}$

FIG·3·4 A STIFFENED PLATE UNDER AXIAL COMPRESSION

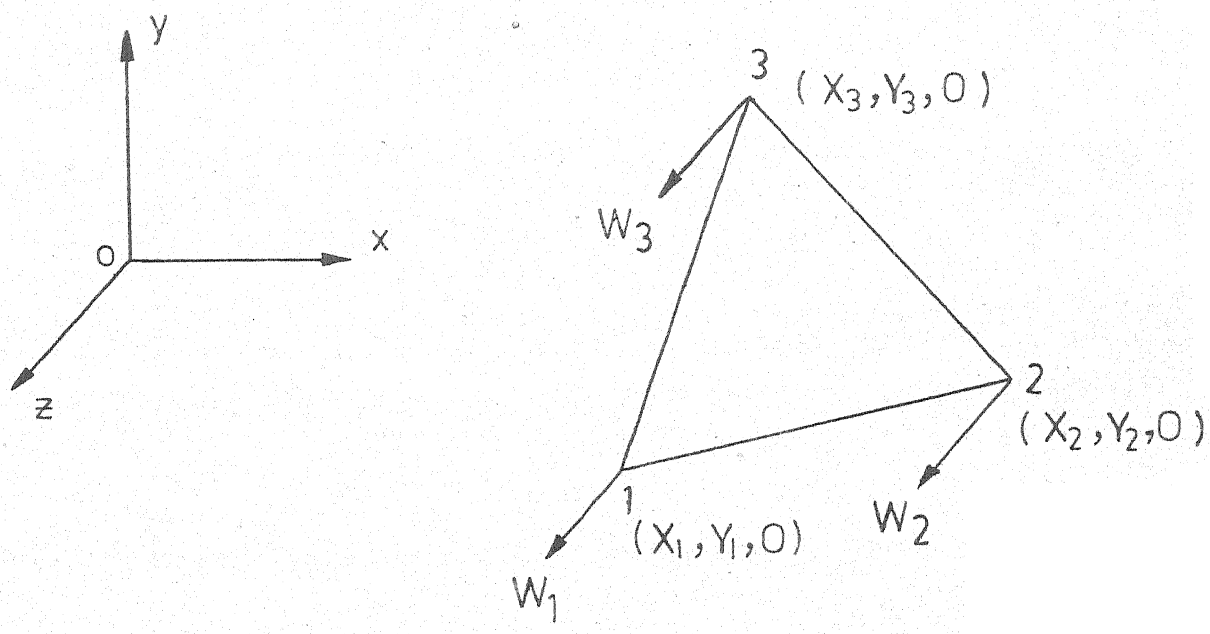

FIG.3.6 A TRIANGULAR ELEMENT IN THE PLANFORM OF THE WING

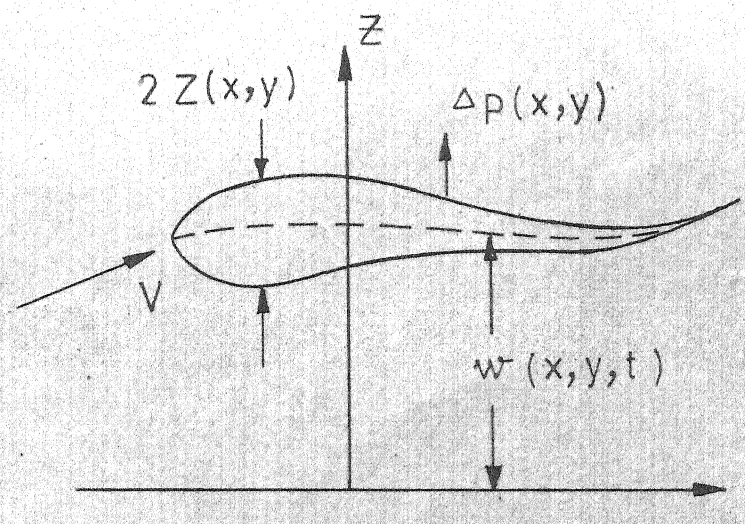

FIG.3.5 AERODYNAMIC LOAD ON A DEFORMED WING

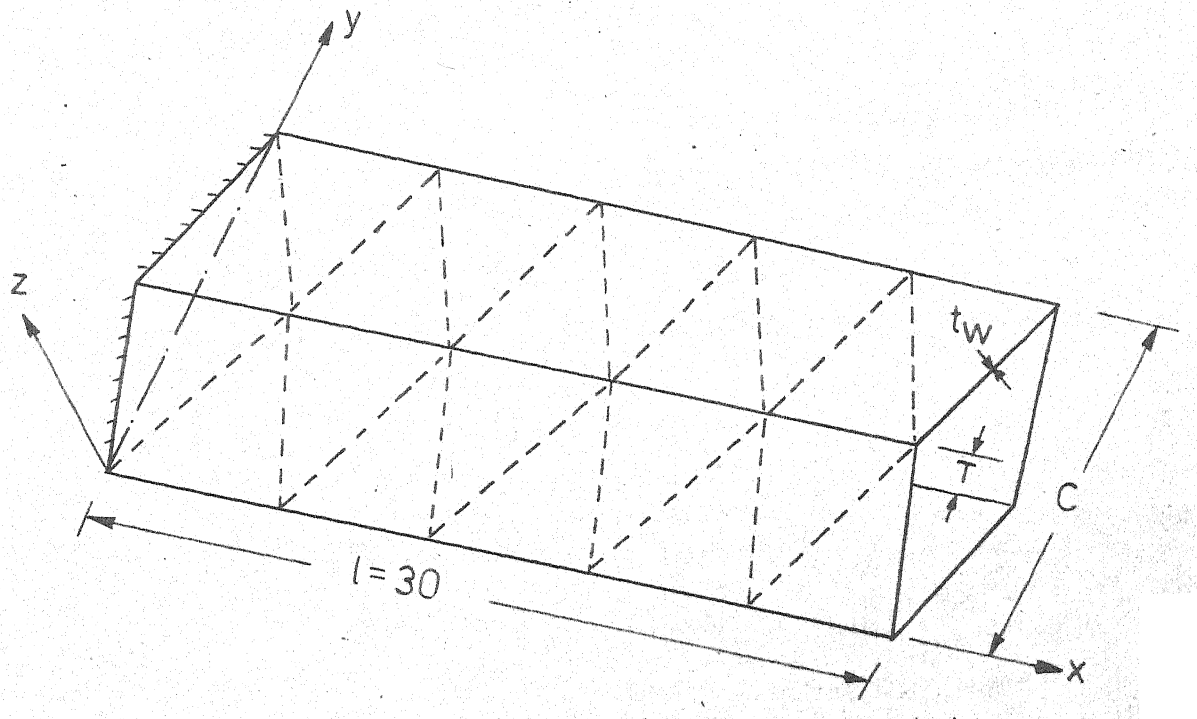

(Dotted lines represent finite element grid)

FIG. 3·7 A DOUBLE WEDGE AIRFOIL

CHAPTER 4

OPTIMIZATION ALGORITHM

The problem of optimum design of aircraft wing structure has been formulated as a nonlinear mathematical programming problem. The selection of solution procedure and its description is presented in this chapter.

The solution procedures of a mathematical programming problem can be classified into (a) Direct methods, in which the constraints are explicifly handled, and (b) Indirect methods, in which the constrained formulation is transformed into a sequence of unconstrained optimizations. One main reason for the appeal of the sequential unconstrained optimization formulation of the constrained optimization problem is that the sequential nature of the method allows a gradual approach to the criticality of the constraints. In addition the sequential approach permits a graded approximation to be used in the analysis of the system. Also this transformation avoids the necessity of coping separately with the boundary of the inequality constrained region, e.g., by attempting to move along the boundary once it is encountered. Such a motion is cumbersome when the constrained surface is nonlinear and it requires the solution of another programming problem to find feasible direction.

One of the approaches to reduce the total computational time of automated optimization problems is to adopt a method which permits the use of approximate analysis without involving significant errors. The penalty function methods allow the use of approximate analysis during the early phases of the optimization. Furthermore the variable metric unconstrained minimization technique, discussed in a later section, is inherently more stable and little effected by minor errors introduced through analysis approximations. It is for this reason that an optimization technique from the indirect methods was choosen for the purpose of the present work.

4.1 Fiacco-McCormick Interior Penalty Function Method

Penalty function methods transform the basic problem into alternative formulations such that numerical solutions are sought by solving a sequence of unconstrained minimization problems. A penalty function $\phi(\vec{X}, r_k)$, will be formulated by adding a penalty term $G(g_1, g_2, \ldots)$, which is a function of the constraints to the objective function $f(\vec{X})$ and this penalty function will be minimized for a sequence of response factors r_k. There are many choices available for the penalty term, however Fiacco-McCormick[33] suggested a simple form $r_k \sum_{j=1}^{m} \frac{1}{g_j}$. In this formulation the penalty term is small at points away from the constraints in the feasible region, but it "blows up" as the constraints are approached.

Then the transformed optimization problem is

Minimize

$$\phi(\vec{X}, r_k) = f(\vec{X}) + r_k \sum_{j=1}^{m} \frac{1}{g_j(\vec{X})} \qquad (4.1)$$

for a decreasing sequence of r_k, $r_{k+1} < r_k$.

The penalty term is not simply defined if $\vec{X}$ is infeasible. In many engineering problems it is not difficult to find an initial feasible point at the expense of large value of $f(\vec{X})$. If there is any difficulty in finding an initial value of $\vec{X}$, the method described in reference 34 could be used to find a feasible starting point. In the present work the feasible starting points are found by a process of trial and error.

Since each of the designs generated by this method lies inside the acceptible region of the design space, the method is classified as an "interior penalty function" formulation. The method tends to generate a sequence of designs which decrease the value of the objective function such that none of the designs in the sequence is critical with respect to the set of inequality constraints. This characteristic makes it possible to use approximate analysis methods during major portions of the optimization procedure[19].

4.2 Davidon-Fletcher-Powell Variable Metric Unconstrained Minimization Method.

The selection of an efficient unconstrained minimization algorithm is extremely important since a sequence of such

minimizations of $\phi(\vec{X}, r_k)$ are to be performed. There is wide choice of algorithms of search. These methods are broadly classified into (a) methods of direct search which use only function values and (b) gradient methods which use the gradients of the function also. In general the gradient methods are more superior to the non-gradient methods since they use more information about the function (namely, the gradients). For this reason the Davidon-Fletcher-Powell variable metric method[36] is used in the present study. This algorithm is probably the most powerful general procedure now known for finding a local unconstrained minimum of a function of many variables.

Given a starting point $\vec{X}_o$ and a possitive definite matrix $[H_o]$, this method seeks the local minimum of $\phi(\vec{X}, r_k)$ by generating a sequence of vectors $\vec{X}_{i+1}$, i=1,2,...

where

$$\vec{X}_{i+1} = \vec{X}_i + \tau^* \vec{S}_i \tag{4.2}$$

and

$$\vec{S}_i = - [H_i] \nabla \phi (\vec{X}_i) \tag{4.3}$$

Thus $\vec{X}_{i+1}$ is the design vector corresponding to the minimum of ϕ-function along the current direction $\vec{S}_i$, $\vec{X}_i$, the starting design vector and τ^* is the minimizing-step length. The i^{th} iteration begins with the determination of the search vector $\vec{S}_i$ according to the relation (4.3).

Prior to begining another cycle in the iteration, the matrix $[H_i]$ is modified to take into account local characteristics of

the ϕ-function inorder to avoid the zig-zag behaviour common to many other minimization techniques. The procedure for the updating of the matrix $[H_i]$ is given in reference 36. The stability of the procedure is insured by preserving the symmetry and the possitive definiteness of $[H_i]$ while it is updated. The positive definiteness of the $[H_i]$ matrix is influenced only by the accuracy with which τ^* is determined. In applying the algorithm, therefore, care must be taken to insure that the $[H_i]$ matrix is not updated with data arising from poor approximation to τ^*. Therefore, whenever $\vec{S}_i^T \nabla\phi_{i+1}$ is large (τ^* is poorly approximated) the one-dimensional minimization algorithm may be reapplied to refine τ^*. If this procedure takes excessive computational effort, (more than 2 or 3 refits) the updating process is skipped (set $[H_{i+1}] = [H_i]$) and the algorithm is continued as before.

4.3 Cubic Interpotation One-Dimensional Search Technique.

Several methods are available for determining the minimization step lengths τ^* in Eq. (4.2). Since most of the effort goes towards the computation of minimization step lengths, the selection of an efficient one-dimensional minimization technique becomes extremely important. An efficient one-dimensional search method which is a natural choice with the variable metric algorithm is the well known cubic interpolation one-dimensional technique[34].

The cubic interpolation technique is essentially a gradient algorithm and the gradients already computed in the variable metric algorithm can readily be used.

The one-dimensional search problem is to find $\tau = \tau^*$ which yields the first local minimum of

$$\phi(\vec{X}_i + \vec{S}_i \tau) \equiv \phi(\tau) \tag{4.4}$$

subject to $0 \leq \tau \leq \bar{\tau}$

where $\bar{\tau}$ is the largest τ for which $\phi(\vec{X}_i + \vec{S}_i \tau)$ lies within the feasible region.

The minimizing step length is given by

$$\tau^* = \tau_B - \frac{\phi'_B + Q - Z}{\phi'_B - \phi'_A + 2Q} (\tau_B - \tau_A) \tag{4.5}$$

where

$$\begin{aligned} \phi(\tau = \tau_A) &= \phi_A \\ \phi(\tau = \tau_B) &= \phi_B \\ \left.\frac{\partial \phi}{\partial \tau}\right|_{\tau = \tau_A} &= \phi'_A \\ \left.\frac{\partial \phi}{\partial \tau}\right|_{\tau = \tau_B} &= \phi'_B \end{aligned} \tag{4.6}$$

and $\phi'_A < 0 < \phi'_B$

also $$Z = \frac{3(\phi_A - \phi_B)}{\tau_B - \tau_A} + \phi'_B + \phi'_A$$

$$Q = [Z^2 - \phi'_A \phi'_B]^{1/2}$$

The effort involved in this algorithm is reaching the points $\tau = A$, and $\tau = B$ satisfying the condition $\phi'_A < 0 < \phi'_B$. If the initial step length is small numerous increases in τ will be necessary before this condition is satisfied. On the other hand if the initial step length is choosen comparatively large, then the interpolation takes place over so large an interval that it produces a poor approximation to τ^*. A simple solution to this problem is to use a priori method which assumes initially that $\phi(\tau)$ can be approximated by a quadratic and then use $\phi(0)$, $\phi'(0)$, and $\bar{\phi}$, a guess at the minimum of ϕ along $\vec{S}$ as the data for interpolation. For ϕ to be minimum, the initial step length can easily be calculated as[34]

$$\tau_o = -2(\phi_o - \bar{\phi})/\phi'_o \tag{4.7}$$

In the present work $\bar{\phi}$ is assumed to be 85% of $\phi(0)$, this being an educated guess.

The one-dimensional interpolation procedure is terminated when the cosine of the angle between $\vec{S}_i$ and $\nabla\phi_{i+1}$ is small.

$$|\cos\theta| = \left| \frac{\vec{S}_i^T \nabla\phi_{i+1}}{|\vec{S}|\,|\nabla\phi_{i+1}|} \right| < \varepsilon(=0.05) \tag{4.8}$$

If this orthogonality test fails, the interpolation is again performed setting

$$\tau_B = \tau^*$$

$$\phi_B = \phi^* \qquad (4.9)$$

$$\phi'_B = \vec{S}_i^T \nabla\phi_{i+1} \quad \text{if} \quad \vec{S}_i^T \nabla\phi_{r+1} > 0$$

otherwise

$$\tau_A = \tau^*$$

$$\phi_A = \phi^* \qquad (4.10)$$

$$\phi_A = \phi^*$$

$$\phi'_A = \vec{S}_i^T \nabla\phi_{i+1}$$

In the present work these refits are limited to a maximum of 5 in each one dimensional search problem.

4.4 Additional Considerations

(1) Starting Point $\vec{X}_o$

The feasible starting point is found by a process of trial and error. Each subsequent stage uses the solution of previous stage as a starting point. In some cases, the overall procedure has been accelerated by employing an extrapolation technique[34] to determine starting points for subsequent unconstrained minimizations. Starting points obtained by extrapolation must be checked to be sure that they satisfy the constraints.

(2) Values of r_k.

If r is very large the function is easy to minimize, but the minimum may lie far from the desired solution to the original

constrained minimization problem. On the otherhand if r is small the function will be hard to minimize. In the present work, the value of r_1 is choosen such that

$$1.25 f(\vec{X}_o) \leq \phi(\vec{X}_o, r_1) \leq 2.00\, f(\vec{X}_o) \tag{4.11}$$

The subsequent values r_{k+1} are found by using the ratio

$$r_{k+1}/r_k = 0.1 \tag{4.12}$$

(3) Termination of minimization for each r_k.

The minimization of $\phi(\vec{X}, r_k)$ for each r_k is terminated when the decrease in penalty function for successive iterations is less than 0.5%. To guard against premature termination due to slow convergence a minimum of N (no. of variables) one dimensional minimizations is performed before testing for convergence. Even after N iterations if the convergence is failed, the [H] matrix is reset to [I] matrix and the minimization process is continued.

(4) Relative minima.

In order to see whether any relative minima exist in the design space, two completely different starting points are used for the sequence of minimizations for one problem. The 2 sequences led to the same optimum design (except for a small difference that might have occured due to numerical instability) and hence it appears that the local optimum is the same as the global optimum for that problem .

(5) Reducing the total computational time.

It has been observed that some of the automated optimum design problems take a longer time to satisfy the prescribed convergence criteria even after reaching very near to the optimum design. This happens whenever the function is highly distorted or eccentric. In such cases it is not worthwhile to try to reach the exact minimum to obtain about 1 or 2% decrease in the objective at the expense of 40 to 50% more computing time. This problem can be tackled by having coarse convergence criteria in the early stages of optimization (initial 'r' s) and later using refined convergence criteria. Also initial unconstrained minimizations produce greater reduction in the objective function and the final unconstrained minimizations produce lesser reduction in the objective function as the design point gets closer to the boundary of the constraints . Thus it may not be profitable to press for a few percent reduction in the later stages of unconstrained minimizations at the cost of substantial computer time (30 to 40%). Hence in the present work only 4 unconstrained minimization are employed for each problem. In such a case testing for the satisfaction of Kuhn-Tucker conditions can be deleated.

Also most of the computer time in the automated optimum design programs is expended in repeat time-consumming design analyses. Hence a rapid reanalysis is the key factor in speeding the optimization program. The behaviour variables can be linearly approximated

whenever the changes in the design variables are small.

Let M_F be the flutter Mach number corresponding to the design $\vec{X}$ and M_F^* be the flutter Mach number corresponding to a perturbed design $\vec{X}^*$. By knowing M_F and the rates of changes of M_F at $\vec{X}$, the flutter Mach number at the perturbed design can be approximated as

$$M_F^* \simeq M_F + \sum_{k=1}^{N} \frac{\partial M_F}{\partial X_K} \Delta x_k \,. \qquad (4.13)$$

provided

$$\frac{\Delta x_k}{X_k} = \frac{X_k^* - X_k}{X_k} < \varepsilon \,, \quad k \in N \qquad (4.14)$$

The value of ε is taken as 0.1 in the early stages of optimization and is successively reduced to 0.02 in the final stages of optimization. A similar procedure is applied to compute the other response variables like natural frequencies, deflections & stresses. It has been observed that this simple approximation alone has resulted in 30% reduction of the total computer time, however with about 2% increase in the final minimum weight.

(6) Partial derivatives.

The partial derivatives of the response variables, weight, natural frequencies, deflection, flutter Mach number are computed using forward finite difference formula, for example,

$$\frac{\partial M_F}{\partial X} = \frac{M_F' - M_F}{X' - X} \qquad (4.15)$$

where M_F' is the flutter Mach number corresponding to the design vector $\vec{X}' = 1.05\vec{X}$.

Although exact expressions for the partial derivatives of the behaviour quantities are available[16], their usage requires additional storage in the computer programme and hence the partial derivatives are computed using the finite difference method.

CHAPTER 5

RESULTS AND DISCUSSIONS

A computer programme packagehas been developed to obtain the minimum weight design of a symmetric wing (airfoil section is of diamond shape) with constant planform area satisfying the require-ments of strength, stability, frequency and flutter (not included in subsequent study). The programme is written in Fortran IV larguage and executed on IBM 7044 computer system. Also a flow chart of the same programme is presented in Appendix B. The dimensions of the wing structure (Fig. 5.1) depend upon the aspect ratio, thickness to chord ratio and sweepback angle which are among the design variables considered. The leading edge and trailing edge spars are assumed to be at 10% and 90% of the chord respectively. Then the main dimensions of the wing can be obtained as

$$b, \text{ semispan} = (AR \cdot SA \cdot 0.5)^{1/2} \qquad (5.1)$$

$$c, \text{ chord} = b \text{ Tan } (SW) + SA/b$$

$$t, \text{ maximum thickness} = (c - 2\, b \text{ Tan } (SW)).\ TR/0.8$$

where

SA = Planform area of the semispan of the wing.

SW = Sweepback angle of the leading edge.

AR = Aspect ratio of the wing.

TR = Thickness to chord ratio of the wing.

The relevent data assumed for the wing is presented in table 5.1.

As shown above, the main dimensions of the wing depend upon design variables and whenever the design is changed, the dimensions are to be re-evaluated.

The finite element idealization of the wing is done with 50 nodes and 172 elements (64 triangular membrane elements, 36 rectangular shear panels and 72 pin-jointed bars). The original 120 degrees of freedom are reduced to 60 using plate flexural assumptions, and these 60 degrees of freedom are further reduced to 20 in the eigen problem by making use of static condensation technique. The flutter constraint is not included in the optimization problem since its double eigenvalue analysis is time consuming and also it requires additional storage in the computer system. To start with 13 design variables - 10 design variables representing the linearly decreasing mass distribution of cover skins, spar webs, rib webs, spar flanges and rib flanges, and 3 more design variables representing the aspect ratio, thickness to chord ratio and sweepback angle were considered. However the results of the initial parametric study (Table 5.2) conducted to observe the influence of the design variables on the behaviour quantities showed that the linearly decreasing mass distribution of spars and ribs can be replaced by uniform distribution without any appreciable change in behaviour constraints, thus reducing the number of design variables to 9. X_1 and X_2 represent the linearly decreasing mass distribution $(X_2 - xX_1)$ of the cover plates; X_3 and X_5 represent the web thicknesses of the spars and ribs,

X_4 and X_6 represent the flange areas of spars and ribs and X_7, X_8, X_9 represent respectively the aspect ratio, thickness to chord ratio and sweepback angle.

The minimum weight design problem is initially solved employing linearly - approximated ~~redesigns~~ reanalyses and the results are given in Table 5.3a. To assess the saving achieved in computational effort by employing the linearly - approximated ~~redesigns~~ reanalyses, the same problem is solved (with the same starting point) using exact analysis in the third and fourth unconstrained minimizations. The results (Table 5.3b) indicate that the total computational time is reduced by about 30% and the minimum weight is increased by about 1.50% when the linearly - approximated ~~redesigns~~ reanalyses are used.

To check whether the optimum obtained is local or global the same problem is solved with a different starting point. The results are presented in Table 5.3c. It is observed that this second starting point gave an 8% over-weight design, suggesting another local optimum. In such a case it is customary to solve the problem from another starting point and obtain some inference regarding the global optimum from the three local optima by using interpolation technique. However this is not attempted in the present investigation.

It can be observed that the optimum structure, in the present case has become stiffer. This can be justified with the argument

that the present idealization reduces it to a Mitchell structure and an optimum Mitchell structure is a stiffer structure.

The results of the parametric study conducted about the optimum point of this problem are presented in Figs. 5.2 to 5.9. These graphs help to evaluate the extent by which one pays the penalty interms of weight if off - design points are considered.

It can be observed from the results (Table 5.3) that only the root buckling stress constraint, and no other side constraint, is active. Normally it is expected that an optimum solution should be a lower bound solution. However, in the present case a wide margin is given on the side constraints, which explains why none of them are active. To check whether the optimization routine is working correctly or not, a second optimization problem is solved with constraints made more stringent. The results of this problem are presented in Table 5.4. The optimum of this problem is characterized by an active frequency constraint and some side constraints.

Further, it can be observed from the results, that minimum weight design of a wing structure is feasible even when the geometric parameters aspect ratio, thickness to chord ratio and sweepback angle are included in the design variables.

TABLE 5.1

DATA FOR EXAMPLE WING

Material properties:	Material	Titanium
	Young's modulus	16.4×10^6 psi
	Poisson's ratio	0.3
	Density	0.16 lb./cu.in
Details of wing loading:	Planform area	3542 sq. ft.
	Pay load	400,000 lb
	Solidity ratio	0.1 (1st problem)
		0.11(2nd problem)
Flight conditions:	Alititude	25,000 ft.
	Density of air	0.0010663 lb - sec^2/ft^4
	Speed of sound	1016.10 ft/sec.
	Flight Mach number	2.5

TABLE 5.2

RESULTS OF INITIAL PARAMETRIC STUDY

o/o Change in Design Variables		o/o Change in Behaviour Quantities							
		f(X) (49.5)	δ_{tip} (44.1)	σ_{Root} (41.8)	σ_{tip} (9.4)	$\sigma_{b.Root}$ (41.0)	$\sigma_{b.tip}$ (8.69)	ω_1 (2.46)	ω_2 (3.95)
X_1 (0.05)	+ 50	- 11.0	+ 8.60	0.000	+ 49.00	0.00	+53.00	+14.70	+8.10
	- 50	+ 11.0	- 3.60	0.000	- 24.10	0.00	-25.40	- 9.35	-5.80
X_2 (0.35)	+ 50	+ 55.0	-35.00	-33.20	- 44.50	-33.30	-45.40	- 6.90	- 4.30
	- 50	- 57.0	+145.00	+96.00	+490.00	+97.00	+520.00	+31.00	+13.20
X_3 (0.05)	+ 50	- 0.2	+0.23	0.00	+ 0.60	0.00	+0.31	+ 0.5	+ 0.17
	- 50	+ 0.2	-0.15	0.00	- 0.32	0.00	-0.23	- 0.15	- 0.25
X_4 (0.35)	+ 50	+ 1.0	-0.68	-0.16	- 0.60	-0.16	-0.54	- 0.27	- 0.42
	- 50	- 1.0	+2.60	0.00	+ 4.60	0.00	+1.65	- 0.54	- 0.25
X_5 (0.2)	+ 50	- 0.40	+0.46	0.00	+ 1.00	0.00	0.62	+ 0.25	- 0.34
	- 50	+ 0.40	-0.30	0.00	- 0.64	0.00	-0.46	- 0.25	-0.51
X_6 (1.4)	+ 50	+ 2.0	-1.36	-0.32	- 1.20	-0.32	-1.10	- 0.54	-0.84
	- 50	- 2.0	+5.2	0.00	+ 9.20	+0.00	+3.30	- 1.08	-0.51
	(1)	(2)	(3)	(4)	(5)	(6)	(7)	(8)	(9)

TABLE 5.2 (contd.)

(1)		(2)	(3)	(4)	(5)	(6)	(7)	(8)	(9)
X_7	+50	-0.1	0.00	0.00	0.00	0.00	0.00	+0.15	+0.08
(0.05)	-50	+0.1	0.00	0.00	0.00	0.00	0.00	-0.15	-0.08
X_8	+50	+0.5	-0.07	0.00	-0.04	0.00	0.00	-0.41	-0.3
(0.35)	-50	-0.5	+0.38	-0.08	+0.11	-0.08	-0.5	+0.41	+0.8
X_9	+50	-0.1	0.00	0.00	0.00	0.00	0.00	+0.25	+0.17
(0.2)	-50	+0.1	0.00	0.00	0.00	0.00	0.00	-0.25	-0.17
X_{10}	+50	1.0	-0.15	0.00	-0.07	0.00	0.00	-0.82	-0.70
(1.4)	-50	-1.0	+0.76	-0.16	+0.21	-0.16	-1.0	+0.82	+0.17
X_{11}	+50	+1.0	+188.00	+60.00	+115.00	+60.00	115.00	-36.6	-13.40
(1.5)	-50	+0.6	- 81.00	-65.00	- 38.40	-65.00	-72.5	+115.00	+48.60
X_{12}	+50	2.4	-55.00	-33.50	-33.00	-33.60	-33.40	+46.4	+46.00
(0.005)	-50	-2.4	+294.00	+101.00	+99.00	101.10	100.00	-48.8	-48.6
X_{13}	+50	+1.8	-13.60	-15.30	+21.30	-15.40	+27.60	+16.70	+ 21.8
(20.0)	-50	-1.4	+19.00	+18.40	- 2.70	+18.50	-16.50	-13.80	-16.50

Note : The quantities in brackets indicate the value of the design variables and behaviour quantities at the initial point. Also X_2-X_1x represents the thickness distribution of cover skins in inches. X_4-X_3x and X_8-X_7x represent the thickness distribution of webs of spars and ribs in inches. X_6-X_5x and $X_{10}-X_9x$ represent the area distribution of flanges of spars and ribs in sq. inches. X_{11}, X_{12} and X_{13} represent respectively the aspect ratio, thickness to chord ratio and sweepback angle.

TABLE 5.3a

OPTIMIZATION RESULTS FOR THE FIRST PROBLEM
(Employs linearly approximated redesigns whenever $\Delta X_i < 0.1$)

Behaviour Quantities	Lower Bounds	Upper Bounds	Initial Design	Sequential Unconstrained Minimizations			
				$r_1=2.9$	$r_2=0.29$	$r_3=0.029$	r
δ (in)	-	69.0	46.0	37.6	36.34	36.34	
σ_{Root} (ksi)	-	75.0	42.0	43.8	49.31	49.31	
σ_{tip} (ksi)	-	75.0	8.03	8.66	9.82	9.82	
$\sigma_{b.Root}$ (ksi)	-	55.0	41.9	43.7	49.19	49.19	
$\sigma_{b.tip}$ (ksi)	-	55.0	7.31	7.97	8.30	8.30	
ω_1 (cps)	1.2	4.5	2.30	2.96	3.45	3.45	
ω_2 (cps)	2.0	7.5	3.80	4.91	5.23	5.23	
Penalty Function			103500	87000	34500	29500	
Weight (lb.)			51900	38300	29100	28990	
Time			about 40 minutes				

* denotes active constraints

TABLE 5.3a (contd.)

Design Variables	Lower Bounds	Upper Bounds	Initial Design	Sequential Unconstrained Minimizations $r_1=2.9$	$r_2=0.29$	$r_3=0.029$
X_1	0.01	0.06	0.035	0.0259	0.0193	0.0193
X_2	0.10	0.60	0.35	0.2590	0.1925	0.1915
X_3	0.10	0.40	0.20	0.1988	0.1750	0.1750
X_4	0.10	0.50	0.35	0.1960	0.2790	0.2785
X_5	0.10	0.40	0.20	0.1988	0.1750	0.1750
X_6	0.10	0.50	0.35	0.1960	0.2790	0.2790
X_7	0.75	3.0	1.50	1.491	1.3120	1.3120
X_8	0.01	0.05	0.015	0.0189	0.0190	0.0190
X_9	10.0	35.0	20.0	21.40	21.50	21.50
Number of one-dimensional minimization for each unconstrained minimization				9	4	2

TABLE 5.3 b

OPTIMIZATION RESULTS FOR THE FIRST PROBLEM

(Employs exact re-analyses in 3rd and 4th uncostrained minimizations)

Behaviour Quantities	Lower Bounds	Upper Bounds	Initial Design	Sequential Unconstrained Minimizations			
				r_1=2.9	r_2=0.29	r_3=0.029	r_4=0.0029
δ (in)	-	69.0	46.0	37.6	36.34	41.7	41.7
σ_{Root} (ksi)	-	75.0	42.0	43.8	49.31	54.4	54.4
σ_{tip} (ksi)	-	75.0	8.03	8.66	9.82	10.5	10.5
$\sigma_{b.Root}$ (ksi)	-	55.0	41.9	43.7	49.19	54.2	54.2*
$\sigma_{b.tip}$ (ksi)	-	55.0	7.31	7.97	8.30	8.96	8.96
ω_1 (cps)	1.2	4.5	2.30	2.96	3.45	3.24	3.24
ω_2 (cps)	2.0	7.5	3.80	4.91	5.23	5.03	5.03
Penalty Function			103500	87000	34500	29100	28380
Weight(lb.)			51900	38300	29100	28300	28300
Total Time			about 60 minutes				

TABLE 5.3b (contd.)

Design Variables	Lower Bounds	Upper Bounds	Initial Design	Sequential Unconstrained Minimations r_1=2.9	r_2=0.29	r_3=0.029	r_4=0.0029
X_1	0.01	0.06	0.035	0.0259	0.0193	0.0188	0.0188
X_2	0.10	0.60	0.35	0.2590	0.1925	0.1880	0.1880
X_3	0.10	0.40	0.2	0.1988	0.1750	0.1818	0.1818
X_4	0.10	0.50	0.35	0.1960	0.2990	0.2780	0.2780
X_5	0.10	0.40	0.20	0.1988	0.1750	0.1820	0.1820
X_6	0.10	0.50	0.35	0.1960	0.2790	0.2780	0.2780
X_7	0.75	3.0	1.50	1.491	1.3120	1.368	1.368
X_8	0.01	0.05	0.015	0.0189	0.0190	0.0191	0.0191
X_9	10.0	35.0	20.0	21.40	21.50	20.20	20.20
Number of one-dimensional minimizations for each unconstrained optimization				9	4	8	2

TABLE 5.3c

OPTIMIZATION RESULTS FOR THE FIRST PROBLEM
(Starting point is different)

Behaviour Quantities		Lower Bounds	Upper Bounds	Initial Design	Sequential Unconstrained Minimizations $r_1=$ 800	$r_2=$ 80	$r_3=$ 8	$r_4=$ 0.8	$r_5=$ 0.08	$r_6=$ 0.008
δ	(in)	-	69.0	39.00	41.08	38.80	39.64	40.29	42.85	42.95
σ_{Root}	(ksi)	-	75.0	45.00	47.01	45.93	48.29	50.71	52.41	52.47
σ_{tip}	(ksi)	--	75.0	8.88	9.07	8.75	8.87	8.79	10.13	10.19
$\sigma_{b.Root}$	(ksi)	-	55.0	44.30	46.87	45.80	48.14	50.55	52.25	52.32
$\sigma_{b.tip}$	(ksi)	-	55.0	7.45	7.72	7.340	7.62	7.56	8.75	8.81
ω_1	(cps)	1.2	4.5	2.92	2.89	2.95	2.97	2.95	3.07	3.08
ω_2	(cps)	2.0	7.5	4.48	4.49	4.58	4.71	4.74	4.83	4.84
Penalty Function					$(x10^6)$ 13.1	12.3	1.275	.158	.046	.0324	.0309
Weight (lb.)					$(x10^3)$ 38.0	36.5	36.0	34.7	33.4	31.2	30.5
Total Time					about 90 minutes						

TABLE 5.3c (contd.)

Design Variables	Lower Bounds	Upper Bounds	Initial Design	Sequential Unconstrained Minimizations r_1= 800	r_2= 80	r_3= 8	r_4= .8	r_5= .08	r_6 = .008
X_1	0.01	0.06	0.042	.029	.028	.024	.019	.025	.025
X_2	0.10	0.60	0.320	.253	.251	.235	.220	.215	.213
X_3	0.10	0.40	0.220	.202	.200	.192	.182	.183	.184
X_4	0.10	0.50	0.210	.213	.210	.215	.214	.212	.213
X_5	0.10	0.40	0.180	.187	.186	.190	.192	.190	.190
X_6	0.10	0.50	0.368	.209	.191	.214	.205	.198	.199
X_7	0.75	3.00	1.350	1.410	1.395	1.430	1.440	1.430	1.43
X_8	0.01	0.05	0.017	.018	.0183	.0189	.0195	.0193	.0192
X_9	10.00	35.00	16.000	17.8	17.5	17.8	17.9	17.8	17.8
Number of one-dimensional minimizations for each unconstrained optimization				9	7	11	4	4	2

TABLE 5.4 a

OPTIMIZATION RESULTS FOR THE SECOND PROBLEM

Behaviour Quantities	Lower Bounds	Upper Bounds	Initial Design	Sequential Unconstrained Minimizations $r_1=0.95$		$r_2=0.095$ $r_3=0.0095$	$r_4=0.00095$
δ (in)	-	47.0	45.96	40.14		41.37	41.37
σ_{Root} (ksi)	-	75.0	42.05	45.66		46.78	46.78
σ_{Tip} (ksi)	-	75.0	8.029	8.968		9.111	9.111
$\sigma_{b.Root}$ (ksi)	-	66.5	41.91	45.54		46.66	46.66
$\sigma_{b.Tip}$ (ksi)	-	66.5	7.311	7.214		7.334	7.334
ω_1 (cps)	1.00	3.00	2.302	2.965		2.93	2.93 *
ω_2 (cps)	3.00	5.00	3.794	4.282		4.250	4.250
Penalty Function			102000	79000		37000	37000
Weight (lb.)			51000	37400		36960	36900
Total Time			About 60 minutes				

Optimization breaks down for this r

TABLE 5.4a (contd.)

Design Variab-	Lower Bounds	Upper Bounds	Initial Design	Sequential Unconstrained Minimizations r_1=0.95	r_2=0.095	r_3=.0095	r_4=0.0095
X_1	0.02	0.04	0.035	0.0253	Optimization breaks from down for this r	0.0250	0.0250
X_2	0.20	0.40	0.35	0.2530		0.250	0.250
X_3	0.15	0.25	0.20	0.1970		0.1932	0.1932
X_4	0.25	0.40	0.35	0.330		0.328	0.328*
X_5	0.15	0.25	0.20	0.1970		0.1932	0.1932*
X_6	0.25	0.4	0.35	0.330		0.328	0.328*
X_7	1.0	2.0	1.50	1.35		1.31	1.31
X_8	0.01	0.03	0.015	0.164		0.0158	0.0158
X_9	15.0	25.0	20.0	19.70		19.20	19.20
Number of one-dimensional minimizations for each unconstrained optimization				9		3	2

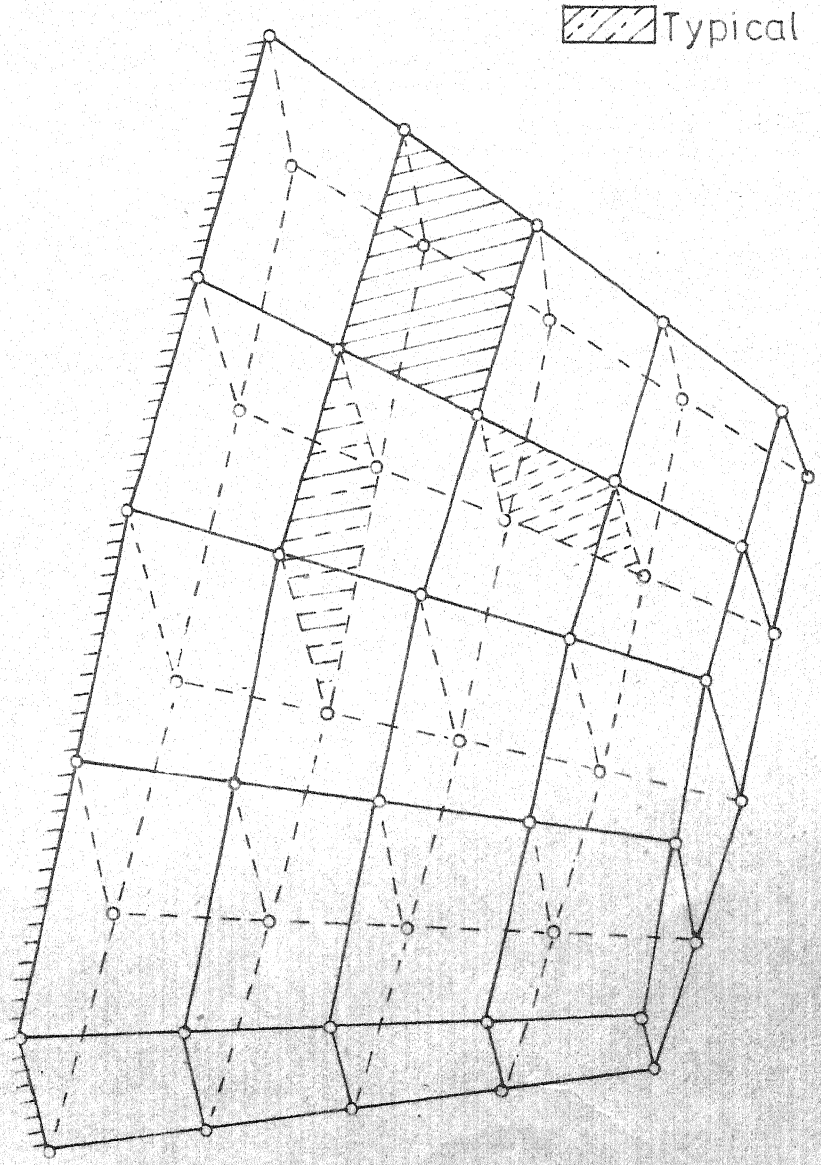

FIG·5·1a WING STRUCTURE IDEALIZATION

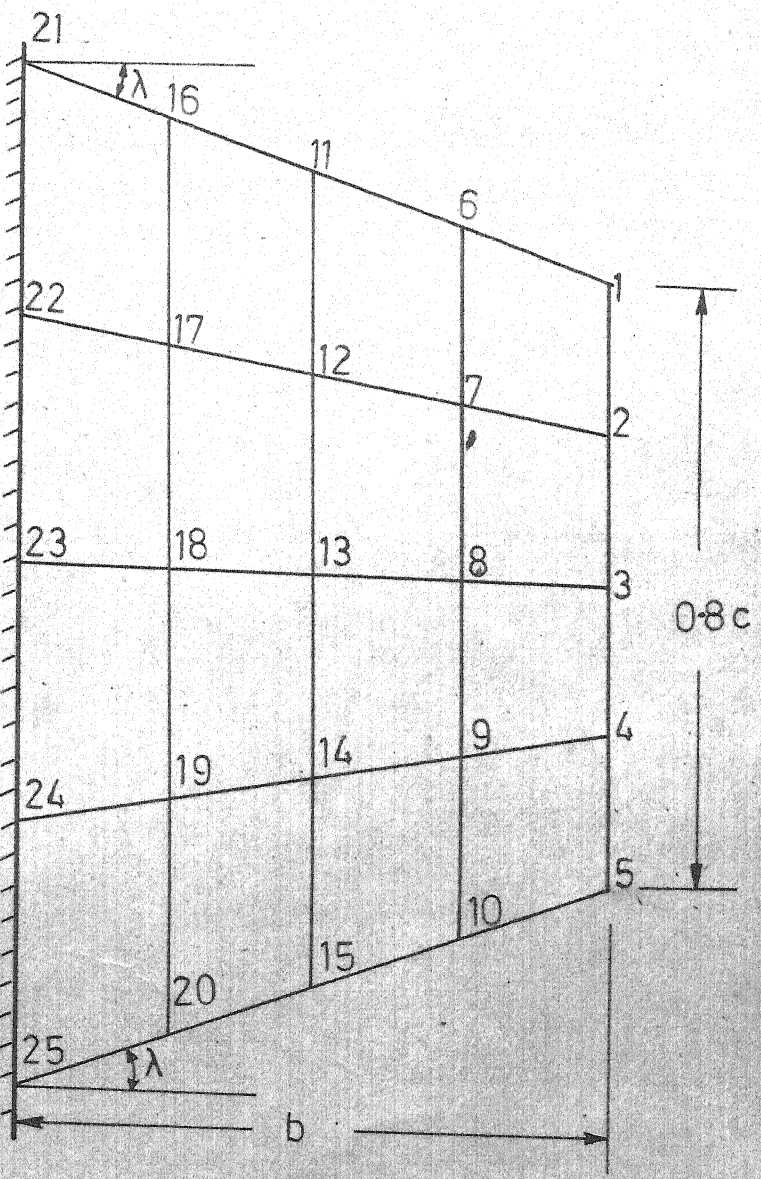

FIG·5·1b PLANFORM NODES AND IMPORTANT DIMENSIONS

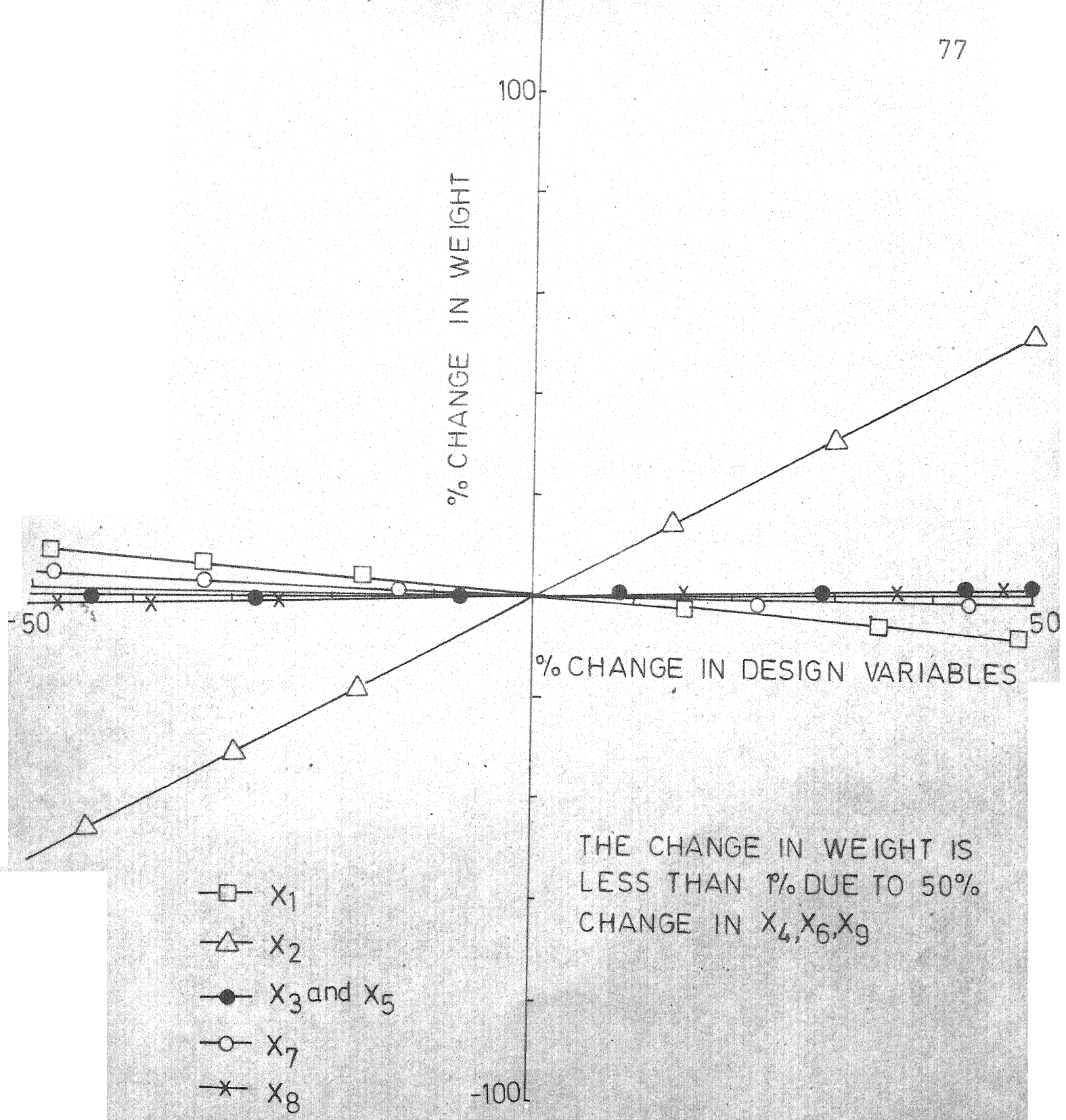

FIG.5.2 VARIATION OF MINIMUM WEIGHT

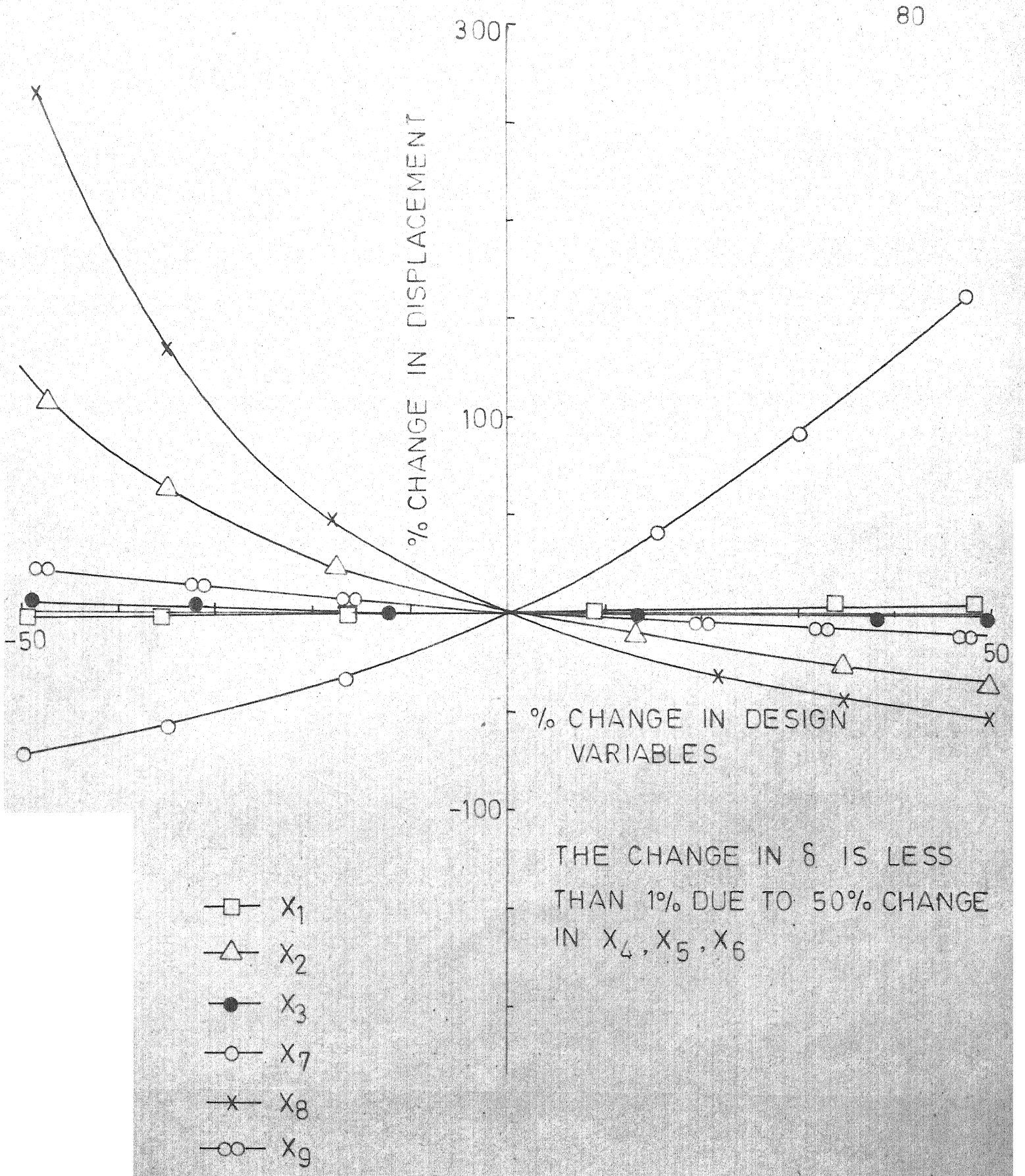

FIG·5·3 VARIATION OF MAXIMUM DISPLACEMENT

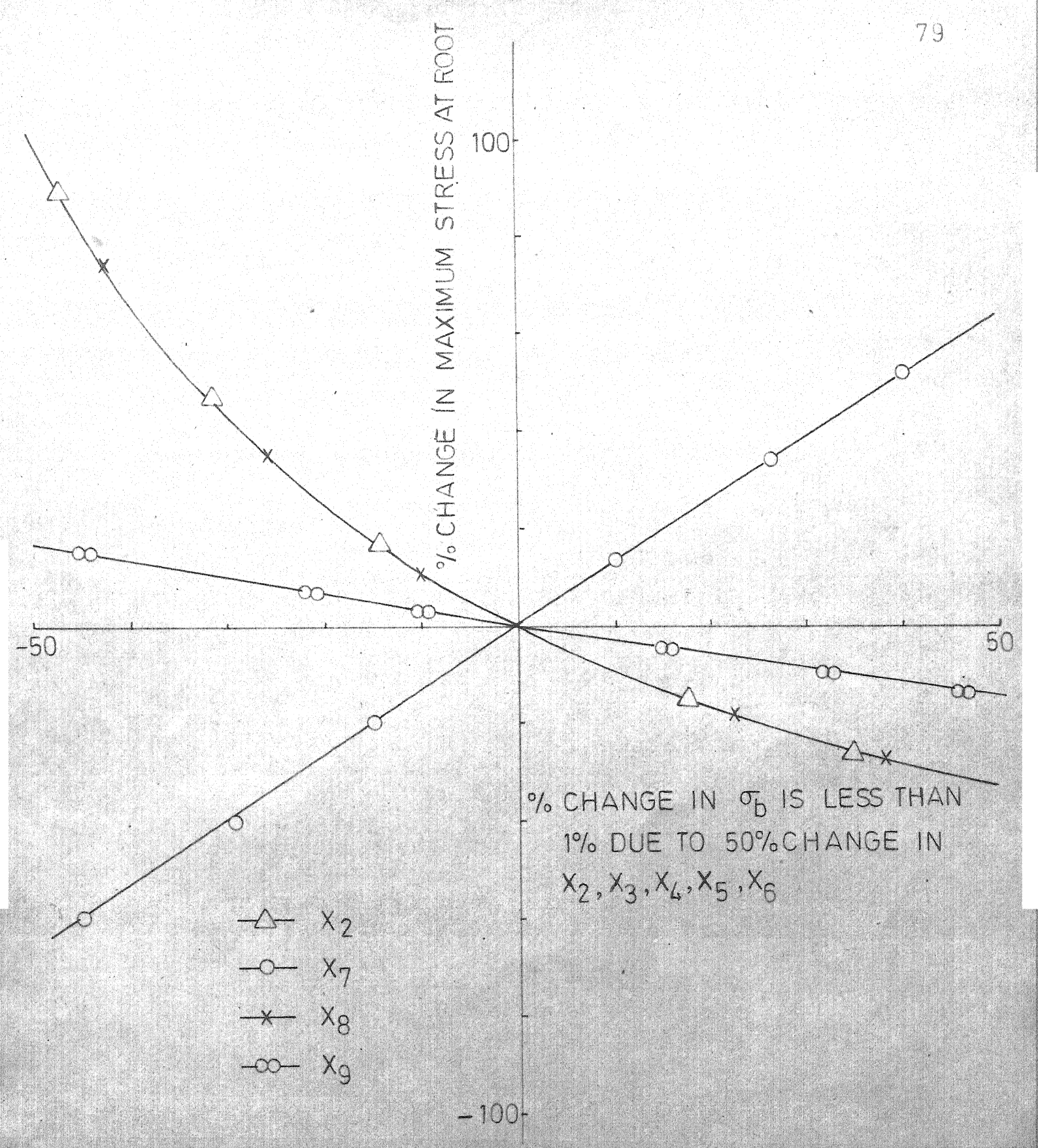

FIG·5·4 VARIATION OF INDUCED STRESS AT ROOT

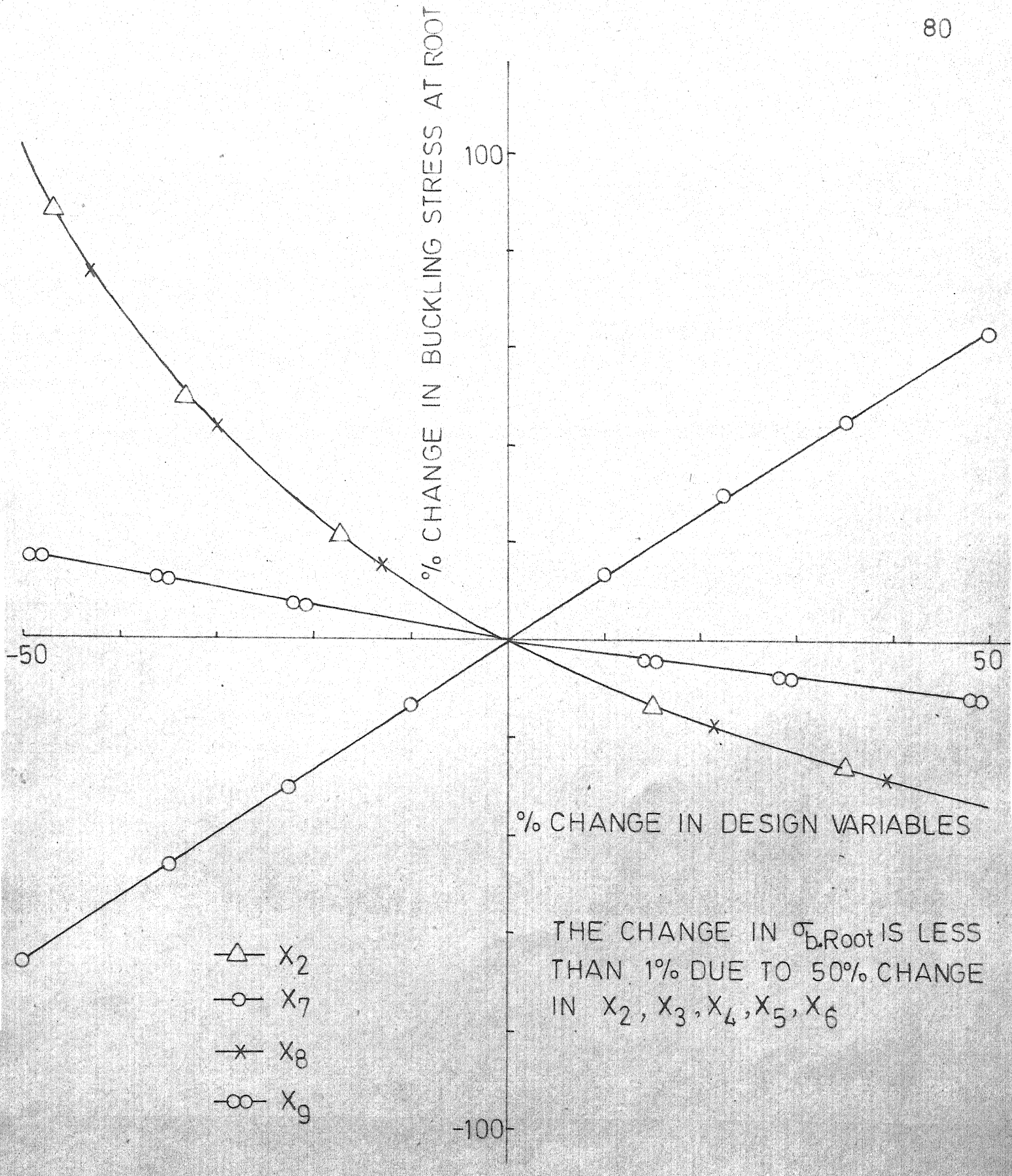

FIG·5·5 VARIATION OF BUCKLING STRESS AT ROOT

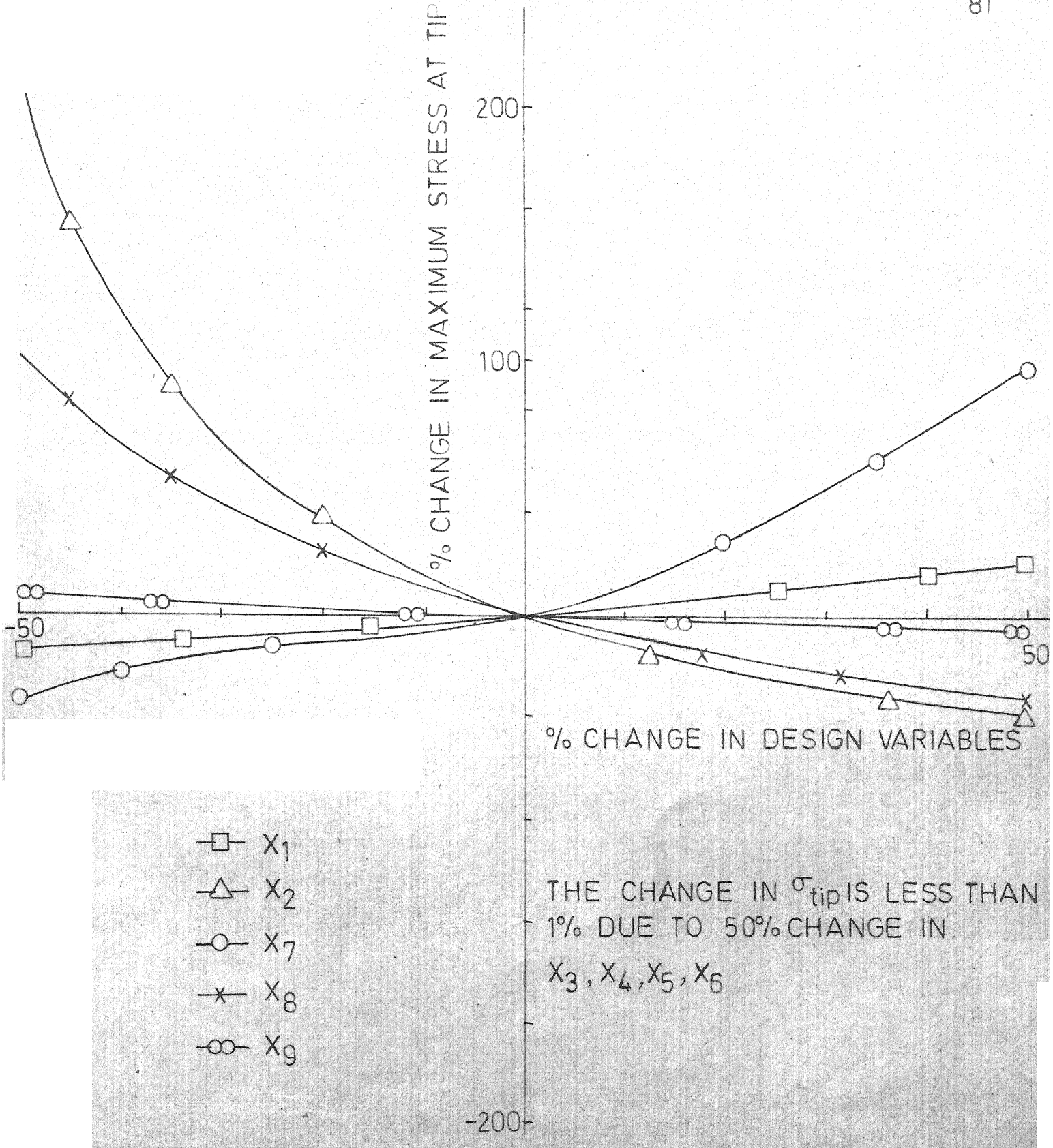

FIG·5·6 VARIATION OF INDUCED STRESS AT TIP

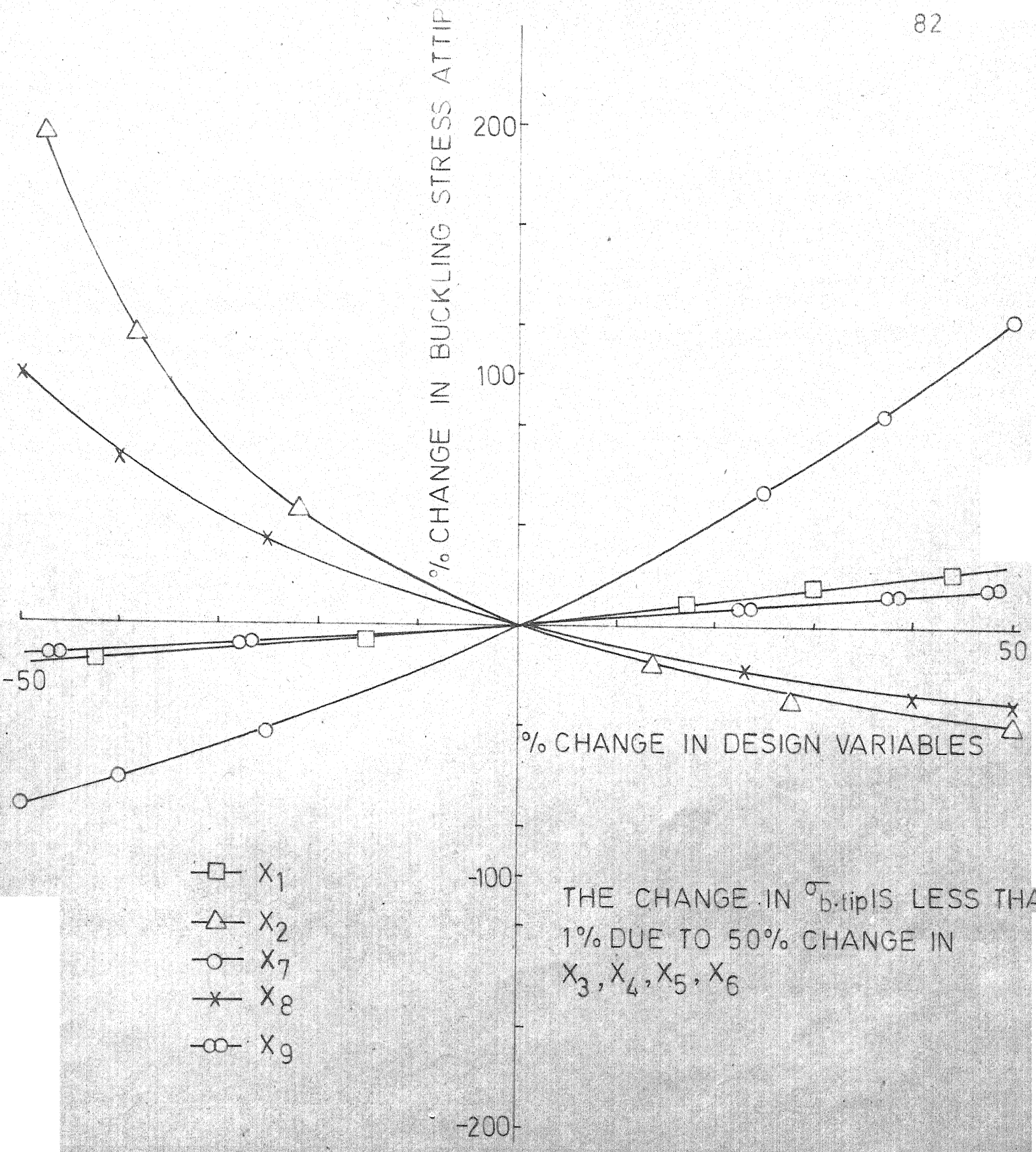

FIG.5·7 VARIATION OF BUCKLING STRESS AT TIP

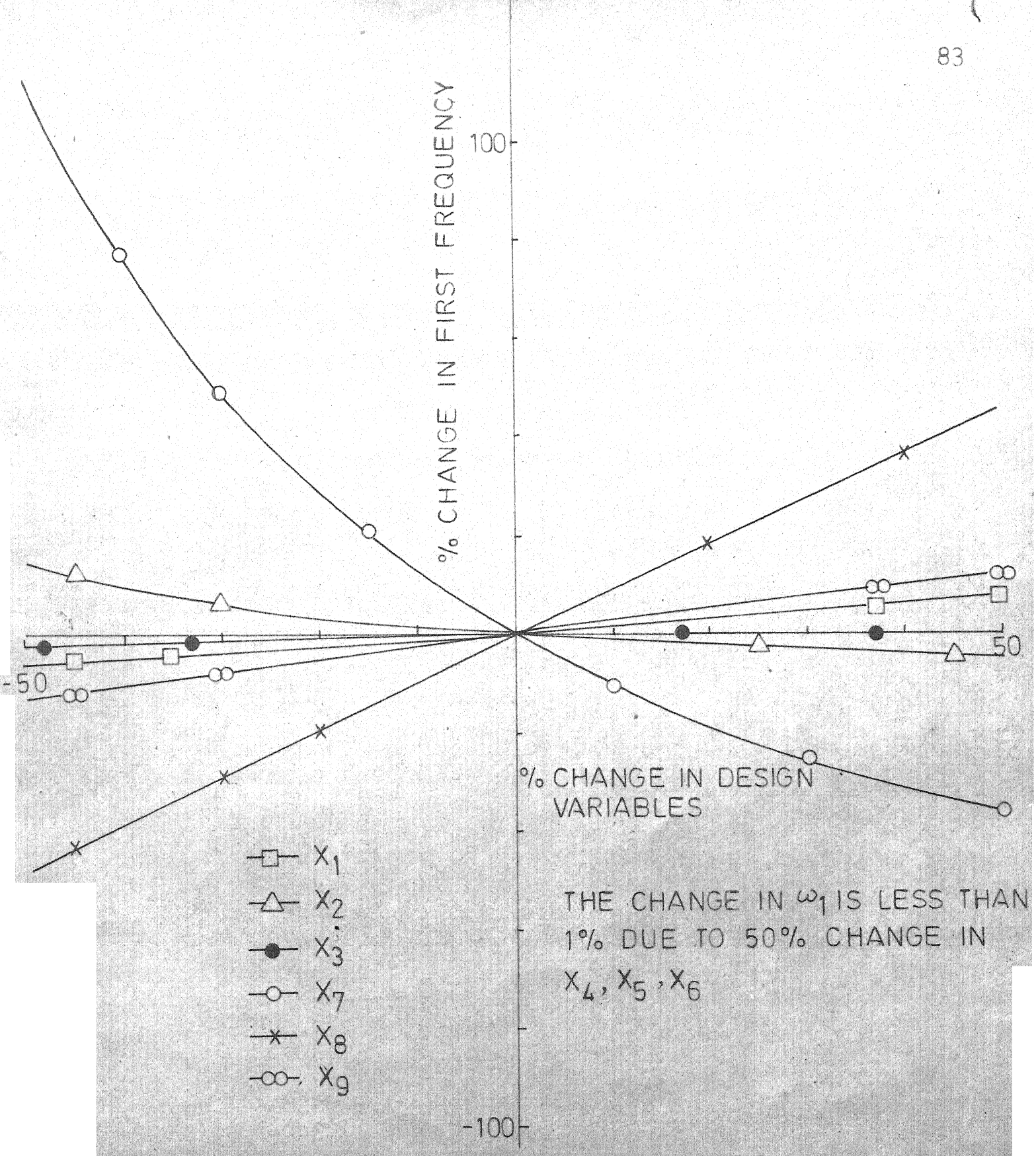

FIG.5·8 VARIATION OF FIRST NATURAL FREQUENCY

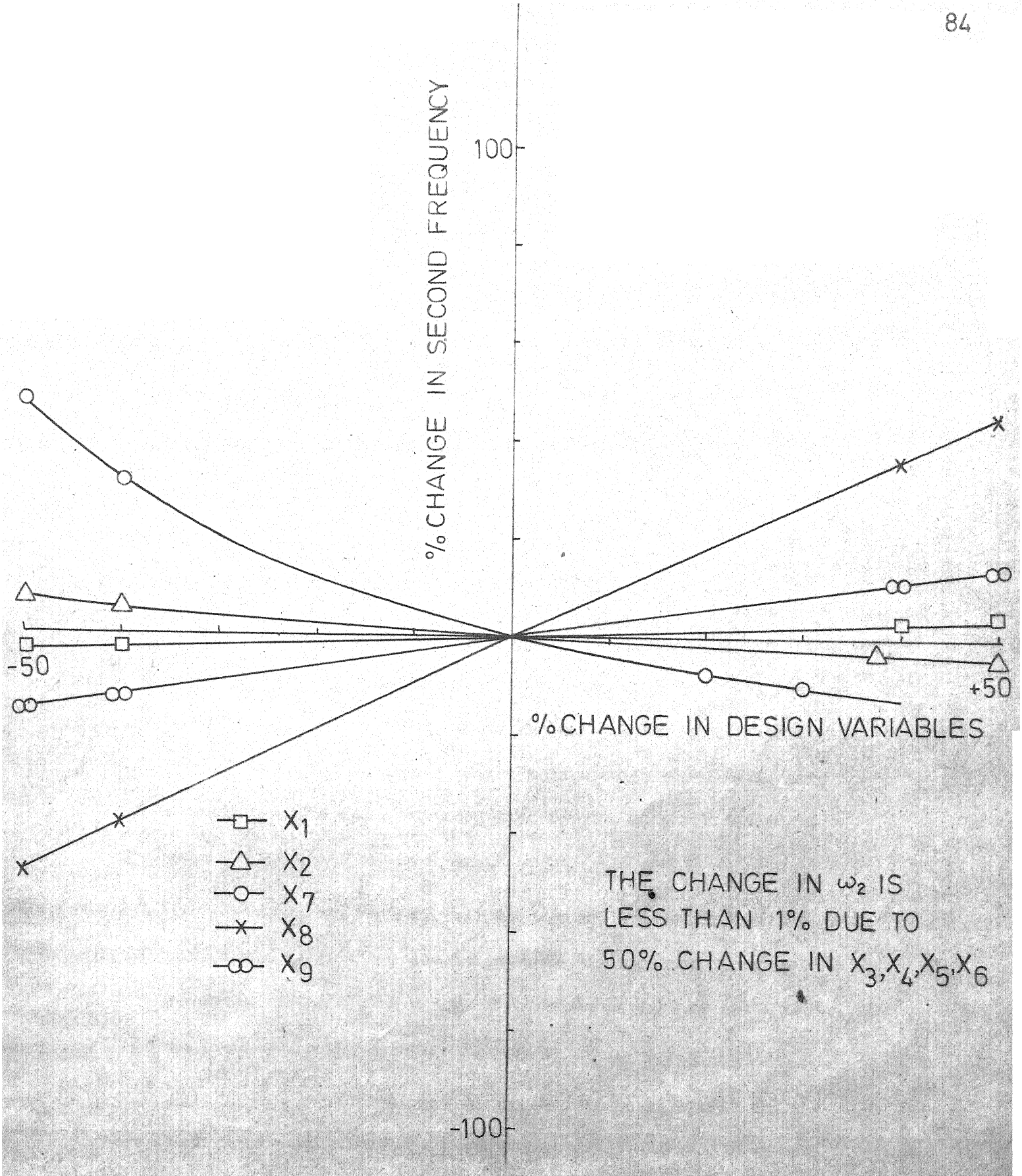

FIG·5·9 VARIATION OF SECOND NATURAL FREQUENCY

(4) The present approach is capable of solving the problem without an undue number of optimization steps. An average of 21 one dimensional minimization steps are required for optimizing a wing with 9 design variables.

(5) The total computational time required for the optimization of one aircraft wing is about 45 minutes. For aircraft, the structural weight saved can be converted directly into increased payload or indirectly into increased range. Hence the computational cost, compared to the reduction in weight obtained, can be seen to be very small. Moreover, designing a wing for strength, stability frequency (and flutter) requirements is certainly better than designing for strength alone and then satisfying the other requirements by making necessary modifications as is being done under the present practice.

(6) In order to represent the behaviour of multiweb wing structures the finite element idealization using triangular membranes, rectangular shear panels and pin-jointed bars has been found to be simple and efficient[16,23]. A reasonably accurate analysis of the structure can be performed even by considering only a fraction of the original degrees of freedom of the structure. The number of degrees of freedom in the static analysis can be reduced by one-half by taking the wing to be symmetric about its middle plane and by using plate fluxural assumptions. The order of the eigen value problem can further be reduced by one-third by employing the static condensation:

technique. The number of degrees of freedom in the flutter analysis can be reduced greatly by using the first few natural modes as generalized coordinates instead of the nodal degrees of freedom.

(7) The total programme is written in such a way that one can use any of the requirements, either strength, stability, natural frequency, flutter and external shape constraints at a time or all of them put together. *

6.2 Recommendations

(1) Several improvements are possible at various stages of the present analysis. In the actual design, the number of degrees of freedom can be increased either by using backup storage or by making use of the theory of substructures. Instead of specifying a fixed-root condition for the wing the flexibility of the fuselage can also be considered in the analysis.

(2) The possibilities of designing the wing under gust loads and landing loads can also be considered. As the aircraft has to pass through various speed zones the unsteady aerodynamic loading can be refined by incorporating an aerodynamics package for subsonic and transponic speed zones as well. Instead of designing the wing for a constant distributed load, the lift load resulting from a given flight condition can be used as design load.

(3) In order to compare the computational time a direct optimization method like Zoutendijk's feasible directions method can be employed for solving the optimization problem. It is to be noted that this method does not offer the flexibility of using approximations in the analysis at several stages.

(4) Since aerodynamic parameters like aspect ratio, sweepback angle are considered as design variables, it is a good caution to guard against drastic changes in the aerodynamic performance by placing constraints on the angle of attack, the lift and drag also.

(5) An obvious extension of the present work is to apply the automated minimum weight design procedure discussed in the present work to complete aircraft structures by treating the entire wing as a substructure and including fuselage, tails etc. This would require additional computer storage and different types of finite elements for proper representation of other structures of aircraft.

---

* CONCLUSIONS - CONTINUED

8. It can also be concluded from the parametric studies that in the initial phase of minimum weight design of ≠ symmetric, thin, low aspect ratio wing structures under bending loads, the mass distribution of spars and ribs can be assumed to be constant, thus reducing the number of variables to be considered for optimization. This will reduce substantially the time required for computation. However, this requires more detailed study before arriving at a decision.

REFERENCES

1. Turner, M.J., "Optimization of structures to Satisfy Flutter Requirements", AIAA Journal, Vol. 7, No. 5, May 1969.

2. Ashley, H., McIntosh, S.C. and Weatherill, W.H., "Optimization under Aeroelastic Constraints". Symposium on Structural Optimization, AGARD Conference Proceedings No. 36, October 1970.

3. Haftka, R.T., "Parametric Constraints with Application to Optimization for Flutter using Continuous Flutter Constraint", AIAA Journal, Vol. 13, No. 4, April 1975.

4. Fox, R.L., and Kapoor, M.P., "Structural Optimization in the Dynamic Response Regime: A Computational Approach", AIAA Journal, Vol. 8, No.10, October 1970.

5. McCart, B.R., Haug, E.J. and Streeter, T.D., "Optimal Design of Structures with Constraints on Natural Frequency" AIAA Structural Dynamics and Aeroelasticity Specialist Conference, New Orleans, April 16-17, 1969.

6. Sippel, D.L., and Warner, W.H., "Minimum-Mass Design of Multi-element Structure under a Frequency Constraint", AIAA Journal, Vol. 11, No. 4, April 1973.

7. Turner, M.J., "Design of Minimum Mass Structures With Specified Natural Frequencies", AIAA Journal, Vol. 5, No. 3, March 1967.

8. Zarghamee, M.S., "Optimum Frequency of Structures", AIAA Journal Vol. 6, No. 4, April 1968.

9. Rubin C.P., "Dynamic Optimization of Complex Structures", AIAA Structural Dynamics and Aeroelasticity Specialist Conference, New Orleans, April 16-17, 1969.

10. Kitcher, T.P., "Structural Synthesis of Integrally Stiffened Cylinders", Journal of Spacecraft and Rockets, Vol. 5, No. 1, January 1968.

11. Zarghamee, M.S., "Minimum Weight Design with Stability Constraint", Journal of Structural Division, Proc. ASCE, Vol. 96, No. ST8, August 1970.

12. Simites, G.J., and Unghbhakorn, V., "Minimum Weight Design of Stiffened Cylinders under Axial Compression", AIAA Journal, Vol. 13, No. 6, June 1975.

13. Schmit, L.A., and Thornton, W A., "Synthesis of an Airfoil at Supersonic Mach Number", NASA CR-144, 1965.

14. Stroud, W.J., Dexter, C.B., and Stein, M., "Automating Preliminary Design of Simplified Wing Structures to satisfy Strength and Flutter Requirements", LWP-961, Langley Research Center, Hampton, May 1971.

15. Giles, G.L., "Procedure for Automating Aircraft Wing Structural Design", Journal of the Structural Division, Proc. ASCE, Vol. 97, No. ST1, January 1971.

16. Rao, S.S., "Automated Optimum Design of Aircraft Wings to Satisfy Strength, Stability, Frequency and Flutter Requirements", Dissertation Submitted in Partial Fulfilment of the Requirements for the Degree of Ph.D. to the Division of Solid Mechanics, Structures and Mechanical Design, Case Westren Reserve University, Cleaveland, 1972.

17. Prager, W., and Taylor J.E., "Problems of Optimum Structural Design", Journal of Applied Mechanics, Vol. 35, March 1968.

18. Shanley, F.R., "Weight Strength Analysis of Aircraft Structures", Dover, New York, 1960.

19. Schmit, L.A., and Pope, G.G., "Structural Design Applications of Mathematical Programming Techniques", AGARD ograph No. 149. Chapter 2, 1971.

20. Pickett Jr., R.M., Rubinstein, M.F., and Nelson, R.B., "Automated Structural Synthesis using a Reduced Number of Design Coordinates", AIAA Journal, Vol. 11, No. 4, April 1973.

21. Pope, G.G., "Optimum Design of Stressed Skin Structures", AIAA Journal, Vol. 11, No. 11, November 1973.

22. Fox, R.L., and Schmit, L.A., "Advances in the Integrated Approach to Structural Synthesis", Journal of Space craft and Rockets, Vol. 3, No. 6, June 1966.

23. Gallagher, R.H., Rattinger, I., and Archer, J.S., "A Correlation study of Methods of Matrix Structural Analysis", The MacMillan Co., New York, 1964.

24. Olson, M.D., "Some flutter solutions using Finite Elements", AIAA Structural Dynamics and Aeroelasticity specialist Conference, New Orleans, April 16-17, 1969.

25. Turner, M.J., Clough, R.W., Martin H.C., and Topp, L.J., "Stiffness and Deflection Analysis of Complex Structures" Journal of Aeronautical Sciences, Vol. 23, No. 9, September 1956.

26. Przemieniecki, J.S., "Theory of Matrix Structural Analysis", McGraw-Hill Book Co., New York, 1968.

27. Timoshenko, S.P., and Gere, J.M., "Theory of Elastic Stability", Second edition, McGraw Hill Book Co., New York, 1961.

28. Crawford, F., "A Theory for the Elastic Deflections of Plates Integrally Stiffened on one Side", NACA TN-3646, 1956.

29. Gerard, G., "Minimum Weight Analysis of Orthotropic Plates under Compressive Loading," Journal of the Aerospace Sciences, Vol. 27, No. 1, January 1960.

30. Bisplinghoff, R.L., Ashley, H., and Halfman, R.L., "Aeroelasticity", Addison-Wesley Publishing Co., Reading, 1955.

31. Morgan, H.G., Huckel, V., and Runyan, H.L., "Procedure for Calculating Flutter at High Supersonic Speed Including Camber Deflections and Comparison with Experimental Results", NACA TN-4335, 1958.

32. Ashley, H. and Zartarian, G., "Piston Theory-A New Aerodynamic tool for the Aeroelastician", Journal of the Aeronautical Sciences, Vol. 23, No. 12, December, 1956.

33. Fiacco, A. and McCormick, G.P., "The Sequential Unconstrained Minimization Technique for Nonlinear Programming. A Primal-Dual Method". Journal of Management Science, Vol. 10, No. 2, January, 1964.

34. Fox, R.L., "Optimization Methods for Engineering Design", Addison-Wesley Publishing Co., Reading, 1971.

35. Pope, G.G., and Schmit, L.A., "Structural Design Applications of Mathematical Programming Techniques", AGARDograph No. 149, Chapter 2, 1971.

36. Fletcher, R. and Powell, M.J.D., "A Rapidly Convergent Descent Method for Minimization" Computer Journal (British), Vol. 6, 1963.

APPENDIX A

Derivation of Element Stiftness and Mass Matrices

The general procedure to be followed in deriving the stiffness and mass matrices of any finite element has been briefly outlined in Chapter 3. The detailed derivation[26] of these matrices from the assumed displacement or stress state will be presented in this appendix for the three types of elements used in the idealization

A - 1. Stiffness Matrix for a Triangular Membrane Element

By assuming a linear variation of the displacement, the inplane displacement functions $u(x,y)$ and $v(x,y)$ for the triangular plate shown in Fig. (A.1) can be presented as

$$u(x,y) = d_1 x + d_2 y + d_3 \tag{A.1}$$

and

$$v(x,y) = d_4 x + d_5 y + d_6 \tag{A.2}$$

where the six arbitrary coefficients $d_1, d_2, \ldots d_6$ can be found from the inplane displacements of the three vertices of the triangle. Using the boundary conditions

$$\begin{aligned} u(x_1,y_1) &= U_1 , \quad v(x_1,y_1) = V_1 \\ u(x_2,y_2) &= U_2 , \quad v(x_2,y_2) = V_2 \\ \text{and} \qquad u(x_3,y_3) &= U_3 , \quad v(x_3,y_3) = V_3 \end{aligned} \tag{A.3}$$

in Eqs. (A.1) and (A.2) to evaluate the unknown coefficients, it can be shown that

$$\begin{Bmatrix} u(x,y) \\ v(x,y) \end{Bmatrix} = \begin{bmatrix} a_{11} & a_{12} & a_{13} & a_{14} & a_{15} & a_{16} \\ a_{21} & a_{22} & a_{23} & a_{24} & a_{25} & a_{26} \end{bmatrix} \begin{Bmatrix} U_1 \\ V_1 \\ U_2 \\ V_2 \\ U_3 \\ V_3 \end{Bmatrix} \qquad (A.4)$$

where

$$a_{11} = a_{22} = \frac{1}{2A_{123}} [(y_3-y_2)(x - x_2) - (x_3- x_2)(y - y_2)]$$

$$a_{13} = a_{24} = \frac{1}{2A_{123}} [(y_1-y_3)(x - x_3) - (x_1- x_3)(y - y_3)] \qquad (A.5)$$

$$a_{15} = a_{26} = \frac{1}{2A_{123}} [(y_2-y_1)(x - x_1) - (x_2- x_1)(y - y_1)]$$

$$a_{12} = a_{14} = a_{16} = a_{21} = a_{23} = a_{25} = 0$$

A_{123}= Area of the triangle 123 $= \frac{1}{2}[x_{32}y_{21} - x_{21}y_{32}]$

x_i and y_i= x and y coordinates of node i in local coordinate system

$x_{ij} = (x_i - x_j)$; $y_{ij} = (y_i - y_j)$

Eqs. (A.4) can now be used to find the relationship between the total strains ε_{xx}, ε_{yy}, ε_{xy} and six displacements $U_1, V_1, \ldots V_3$. Differentiating these equations, we have

$$\begin{Bmatrix} \varepsilon_{xx} \\ \varepsilon_{yy} \\ \varepsilon_{xy} \end{Bmatrix} = \begin{Bmatrix} \frac{\partial u}{\partial x} \\ \frac{\partial v}{\partial y} \\ \frac{\partial u}{\partial y} + \frac{\partial v}{\partial x} \end{Bmatrix} = \frac{1}{2A_{123}} \begin{bmatrix} y_{32} & 0 & y_{13} & 0 & y_{21} & 0 \\ 0 & x_{23} & 0 & x_{31} & 0 & x_{12} \\ x_{23} & y_{32} & x_{31} & y_{13} & x_{12} & y_{21} \end{bmatrix} \begin{Bmatrix} U_1 \\ V_1 \\ U_2 \\ V_2 \\ U_3 \\ V_3 \end{Bmatrix} \quad (A.6)$$

The stress-strain relation for the case of plane stress is given by

$$\begin{Bmatrix} \sigma_{xx} \\ \sigma_{yy} \\ \sigma_{xy} \end{Bmatrix} = \frac{E}{1-\nu^2} \begin{bmatrix} 1 & \nu & 0 \\ \nu & 1 & 0 \\ 0 & 0 & \frac{1-\nu}{2} \end{bmatrix} \begin{Bmatrix} \varepsilon_{xx} \\ \varepsilon_{yy} \\ \varepsilon_{xy} \end{Bmatrix} \quad (A.7)$$

where E and ν are Young's modulus and Poisson's ratio of the material.

The assumed displacement state satisfies the strain compatibility and the stress equilibrium equations within the element[26]. It can also be seen that the compatibility of displacements on two adjacent triangular elements with a common boundary is ensured. If Eqs. (A.4), (A.6) and (A.7) are written in the matrix form

$$\begin{aligned} \vec{u} &= [a]\ \vec{U} \\ \vec{\varepsilon} &= [b]\ \vec{U} \\ \text{and} \quad \vec{\sigma} &= [c]\ \vec{\varepsilon} \end{aligned} \quad (A.8)$$

the matrices [a], [b] & [c] can be identified from the equations (A.4), (A.6) and (A.7) respectively.

The element stiffness matrix in local coordinate system can be obtained by evaluating the integral in (Eq. (3.10))

$$[k] = \int_{\bar{v}} [b]^T [c] [b] \, d\bar{v} \qquad (A.9)$$

The resulting matrix can be separated into two parts

$$[k] = [k_n] + [k_s] \qquad (A.10)$$

where $[k_n]$ represents the stiffness matrix due to normal stresses, and $[k_s]$ represents the stiffness due to shearing stresses. The two component matrices, as derived from Eq. (A.9) are given by Eqs. (A.11) and (A.12)

$$[k_n] = \frac{Et}{4A_{123}(1-\nu^2)} \begin{bmatrix} y_{32}^2 & & & & & \\ -\nu y_{32}x_{32} & x_{32}^2 & & & \text{Symmetric} & \\ -y_{32}y_{31} & \nu x_{32}y_{31} & y_{31}^2 & & & \\ \nu y_{32}x_{31} & -x_{32}x_{31} & -\nu y_{31}x_{31} & x_{31}^2 & & \\ y_{32}y_{21} & -\nu x_{32}y_{21} & -y_{31}y_{21} & \nu x_{31}y_{21} & y_{21}^2 & \\ -\nu y_{32}x_{21} & x_{32}x_{21} & \nu y_{31}x_{21} & -x_{31}x_{21} & -\nu y_{21}x_{21} & x_{21}^2 \end{bmatrix} \qquad (A.11)$$

$$[k_s] = \frac{Et}{8A_{123}(1+\nu)} \begin{bmatrix} x_{32}^2 & & & & & \\ -x_{32}y_{32} & y_{32}^2 & & & & \\ -x_{32}x_{31} & y_{32}x_{31} & x_{31}^2 & & & \\ x_{32}y_{31} & -y_{32}y_{31} & -x_{31}y_{31} & y_{31}^2 & & \\ x_{32}x_{21} & -y_{32}x_{21} & -x_{31}x_{21} & y_{31}x_{21} & x_{21}^2 & \\ -x_{32}y_{21} & y_{32}y_{21} & x_{31}y_{21} & -y_{31}y_{21} & -x_{21}y_{21} & y_{21}^2 \end{bmatrix} \qquad (A.12)$$

where t is the thickness of the plate element.

Eq. (A.10) gives the stiffness matrix in local coordinate system (x,y). If the element is referred to some global coordinate system $(\bar{x},\bar{y})$ as shown in Fig. (A.2), the new element stiffness matrix is given by

$$\underset{9\times9}{[\bar{k}]} = \underset{9\times6}{[\lambda]^T}\ \underset{6\times6}{[k]}\ \underset{6\times9}{[\lambda]} \tag{A.13}$$

where $[\lambda]$ is a transformation matrix that relates the nodal displacements of the local coordinate system $\vec{\bar{U}}$ with those of global system $\vec{U}$ by

$$\underset{6\times1}{\vec{U}} = \underset{6\times9}{[\lambda]}\ \underset{9\times1}{\vec{\bar{U}}} \tag{A.14}$$

For the triangular membrane element, the matrix $[\lambda]$ is given by[26]

$$[\lambda] = \begin{bmatrix} \ell_{41} & m_{41} & n_{41} & 0 & 0 & 0 & 0 & 0 & 0 \\ \ell_{12} & m_{12} & m_{12} & 0 & 0 & 0 & 0 & 0 & 0 \\ 0 & 0 & 0 & \ell_{41} & m_{41} & n_{41} & 0 & 0 & 0 \\ 0 & 0 & 0 & \ell_{12} & m_{12} & n_{12} & 0 & 0 & 0 \\ 0 & 0 & 0 & 0 & 0 & 0 & \ell_{41} & m_{41} & n_{41} \\ 0 & 0 & 0 & 0 & 0 & 0 & \ell_{12} & m_{12} & n_{12} \end{bmatrix} \tag{A.15}$$

where

$$\ell_{12} = (\bar{x}_2 - \bar{x}_1)/d_{12},\quad m_{12} = (\bar{y}_2 - \bar{y}_1)/d_{12},\quad n_{12} = (\bar{z}_2 - \bar{z}_1)/d_{12}$$

$$d_{12} = [(x_2 - x_1)^2 + (y_2 - y_1)^2 + (z_2 - z_1)^2]^{1/2}$$

$$\ell_{41} = (\bar{x}_3 - \bar{x}_1 - \ell_{12}d_{14})/d_{43}$$

$$
\begin{aligned}
m_{41} &= (\bar{y}_3 - \bar{y}_1 - m_{12} d_{14})/d_{43} \\
n_{41} &= (\bar{z}_3 - \bar{z}_1 - n_{12} d_{14})/d_{43} \\
d_{14} &= \ell_{12}(\bar{x}_3 - \bar{x}_1) + m_{12}(\bar{y}_3 - \bar{y}_1) + n_{12}(\bar{z}_3 - \bar{z}_1) \\
d_{43} &= [(\bar{x}_3 - \bar{x}_1)^2 + (\bar{y}_3 - \bar{y}_1)^2 + (\bar{z}_3 - \bar{z}_1)^2 - d_{14}^2]^{1/2}
\end{aligned}
\qquad (A.16)
$$

A.2 Equivalent Mass Matrix for a Triangular Membrane Element

The equivalent matrix for the element in local coordinate system is given by (Eq. (3.11))

$$
[m] = \int_{\bar{V}} \rho [a]^T [a] \, d\bar{v} \qquad (A.17)
$$

where ρ is the density of the element and $[a]$ has been defined in the Eq. (A.4).

It can be shown[26] that for triangular plates undergoing essentially translational displacements (no bending involved), the mass matrix $[m]$ is invariant with respect to the coordinate transformation. Hence the element mass matrix for a traingular membrane element can be, obtained from Eqs. (A.17) and (A.4) as

$$
[m]_{9\times 9} = [\bar{m}]_{9\times 9} = \frac{\rho A_{123} t}{12}
\begin{bmatrix}
2 & 0 & 0 & 1 & 0 & 0 & 1 & 0 & 0 \\
0 & 2 & 0 & 0 & 1 & 0 & 0 & 1 & 0 \\
0 & 0 & 2 & 0 & 0 & 1 & 0 & 0 & 1 \\
1 & 0 & 0 & 2 & 0 & 0 & 1 & 0 & 0 \\
0 & 1 & 0 & 0 & 2 & 0 & 0 & 1 & 0 \\
0 & 0 & 1 & 0 & 0 & 2 & 0 & 0 & 1 \\
1 & 0 & 0 & 1 & 0 & 0 & 2 & 0 & 0 \\
0 & 1 & 0 & 0 & 1 & 0 & 0 & 2 & 0 \\
0 & 0 & 1 & 0 & 0 & 1 & 0 & 0 & 2
\end{bmatrix}
\qquad (A.18)
$$

A.3 Stiffness Matrix for a Rectangular Shear Panel

For the purpose of present analysis, the trapezoidal shear panel is approximated by an equivalent rectangular shear panel as shown in Fig. (A.3). By assuming a linear stress distribution with in the rectangle 1234

$$\vec{\sigma} = \begin{Bmatrix} \sigma_{xx} \\ \sigma_{yy} \\ \sigma_{xy} \end{Bmatrix} = \begin{Bmatrix} d_1 + d_2 y \\ d_3 + d_4 x \\ d_5 \end{Bmatrix} \tag{A.19}$$

where $d_1, \ldots d_5$ are constants, the displacement field $\vec{u}$ can be derived from the Hooke's law

$$\vec{\sigma} = [c] \vec{\epsilon} \tag{A.20}$$

where $[c]$ has been defined in the Eq. (A.7)

From eqs. (A.19) and (A.20), we obtain

$$\frac{\partial u}{\partial x} = \frac{1}{E}(d_1 + d_2 y - \nu d_3 - \nu d_4 x) \tag{A.21}$$

$$\frac{\partial v}{\partial y} = \frac{1}{E}(d_3 + d_4 x - \nu d_1 - \nu d_2 y) \tag{A.22}$$

$$\frac{\partial u}{\partial y} + \frac{\partial v}{\partial x} = 2(1+\nu)\frac{d_5}{E} \tag{A.23}$$

The solution of Eqs. (A.21) through (A.23) can be given as

$$u(x,y) = \frac{1}{E}\left[d_1 x + d_2 xy - \nu d_3 x - \nu d_4 \frac{x^2}{2} - \frac{d_4 y^2}{2} + d_6 y + d_7\right] \tag{A.24}$$

$$v(x,y) = \frac{1}{E}\left[-\nu d_1 y - \frac{\nu d_2 y^2}{2} - \frac{d_2 x^2}{2} + d_3 y + d_4 xy + 2(1+\nu)d_5 x - d_6 x + d_8\right] \tag{A.25}$$

The unknown constants $d_1, d_2, \ldots d_8$ can be determined from the element displacements $\vec{U}$ and $\vec{V}$. The resulting strain displacement relation, specialized for the case of a shear panel, can be expressed as

$$\vec{\epsilon} = [b] \vec{U} \tag{A.26}$$

where

$$[b] = \begin{bmatrix} 0 & 0 & 0 & 0 & 0 & 0 & 0 & 0 \\ 0 & 0 & 0 & 0 & 0 & 0 & 0 & 0 \\ -\frac{1}{2b} & -\frac{1}{2a} & \frac{1}{2b} & -\frac{1}{2a} & \frac{1}{2b} & \frac{1}{2a} & -\frac{1}{2b} & \frac{1}{2a} \end{bmatrix} \tag{A.27}$$

By using Eqs. (A.7) and (A.27) in Eq. (A.9) the stiffness matrix for a rectangular shear panel in local coordinate system can be evaluated and its final form is given by Eq. (A.28)

$$[K] = \frac{Gt}{4} \begin{bmatrix} \frac{a}{b} & & & & & & & \\ 1 & \frac{b}{a} & & & & & & \\ -\frac{a}{b} & -1 & \frac{a}{b} & & & & & \\ 1 & \frac{b}{a} & -1 & \frac{b}{a} & & & & \\ -\frac{a}{b} & -1 & \frac{a}{b} & -1 & \frac{a}{b} & & & \\ -1 & -\frac{b}{a} & 1 & -\frac{b}{a} & 1 & \frac{b}{a} & & \\ \frac{a}{b} & 1 & -\frac{a}{b} & 1 & -\frac{a}{b} & -1 & \frac{a}{b} & \\ -1 & -b/a & 1 & -b/a & -1 & b/a & -1 & b/a \end{bmatrix} \tag{A.28}$$

where G is the shear modulus of the rectangular plate and $\frac{a}{b}$ is the aspect ratio.

The stiffness matrix of the element with respect to any global coordinate system $(\bar{x},\bar{y},\bar{z})$ can be obtained from

$$\underset{12\times12}{[\bar{k}]} = \underset{12\times8}{[\lambda]^T} \quad \underset{8\times8}{[k]} \quad \underset{8\times12}{[\lambda]}$$

where the transformation matrix $[\lambda]$ is given by

$$[\lambda] = \begin{bmatrix}
\ell_{23} & m_{23} & n_{23} & 0 & 0 & 0 & 0 & 0 & 0 & 0 & 0 & 0 \\
\ell_{12} & m_{12} & n_{12} & 0 & 0 & 0 & 0 & 0 & 0 & 0 & 0 & 0 \\
0 & 0 & 0 & \ell_{23} & m_{23} & n_{23} & 0 & 0 & 0 & 0 & 0 & 0 \\
0 & 0 & 0 & \ell_{12} & m_{12} & n_{12} & 0 & 0 & 0 & 0 & 0 & 0 \\
0 & 0 & 0 & 0 & 0 & 0 & \ell_{23} & m_{23} & n_{23} & 0 & 0 & 0 \\
0 & 0 & 0 & 0 & 0 & 0 & \ell_{12} & m_{12} & n_{12} & 0 & 0 & 0 \\
0 & 0 & 0 & 0 & 0 & 0 & 0 & 0 & 0 & \ell_{23} & m_{23} & n_{23} \\
0 & 0 & 0 & 0 & 0 & 0 & 0 & 0 & 0 & \ell_{12} & m_{12} & n_{12}
\end{bmatrix} \tag{A.30}$$

$$\begin{aligned}
\ell_{ij} &= (\bar{x}_i - \bar{x}_j)/d_{ij} \\
m_{ij} &= (\bar{y}_i - \bar{y}_j)/d_{ij} \\
n_{ij} &= (\bar{z}_i - \bar{z}_j)/d_{ij}
\end{aligned} \tag{A.31}$$

and $$d_{ij} = [(\bar{x}_i - \bar{x}_j)^2 + (\bar{y}_i - \bar{y}_i)^2 (\bar{z}_i - \bar{z}_j)^2]^{1/2}$$

It is to be noted that the assumed stress distribution Eq. (A.19) satisfies the stress equilibrium equations within the rectangle. However, the resulting displacement distribution , Eqs. (A.24) and (A.25) violates the compatibility of boundary displacements on adjacent elements.

A.4 Lumped Mass Matrix for a Rectangular Shear Panel

The equivalent mass matrix of a rectangular shear panel is given by the relation

$$[m] = \int_{\bar{V}} \rho [a]^T [a] \, d\bar{v} \qquad (A.32)$$

where the matrix [a] can be obtained from Eqs. (A. 24) and (A.25). However, the lumped mass matrix of the equivalent rectangular plate shown in Fig. (A.3) is used for the trapezoidal shear panel also as an approximation. It is given by

$$[m] = \frac{\rho abt}{4} \begin{bmatrix} 1 & & & & & & & & & & & \\ & 1 & & & & & & & & & & \\ & & 1 & & & & & & & & & \\ & & & 1 & & & & & & & & \\ & & & & 1 & & & & & & & \\ & & & & & 1 & & & & & & \\ & & & & & & 1 & & & & & \\ & & & & & & & 1 & & & & \\ & & & & & & & & 1 & & & \\ & & & & & & & & & 1 & & \\ & & & & & & & & & & 1 & \end{bmatrix}$$

where

a is the depth of the element and b is the span.

A.5 Stiffness Matrix for a Pin-Jointed Bar Element.

A pin-jointed bar is a one-dimensional element for which the assumed displacement can be taken as [see Fig. (A.4)]

$$\vec{u}(x) = [a]\ \vec{U} = \left[\left(1 - \frac{x}{\ell}\right)\ \ \frac{x}{\ell}\right]\begin{Bmatrix} U_1 \\ U_2 \end{Bmatrix} \tag{A.34}$$

where ℓ is the of the bar.

$$\vec{\varepsilon} = \{\varepsilon_{xx}\} = \left\{\frac{\partial u}{\partial x}\right\} = \left[-\frac{1}{\ell}\ \ \frac{1}{\ell}\right]\begin{Bmatrix} U_1 \\ U_2 \end{Bmatrix} \tag{A.35}$$

and

$$\vec{\sigma} = \{\sigma_{xx}\} = [c]\,\vec{\varepsilon} = E\,\{\varepsilon_{xx}\} \tag{A.36}$$

The element stiffness matrix in local coordinate system is given by

$$\underset{2\times 2}{[k]} = \int_{\bar{V}} [b]^T [c]\ [b]\, d\bar{v} = \frac{AE}{\rho}\begin{bmatrix} 1 & -1 \\ -1 & 1 \end{bmatrix} \tag{A.37}$$

where A is the cross-sectional area of the bar.

Here, the nodal displacements in local and global coordinate systems are related by

$$\vec{U} = [\lambda]\,\vec{\bar{U}} \equiv \begin{bmatrix} \ell_{12} & m_{12} & n_{12} & 0 & 0 & 0 \\ 0 & 0 & 0 & \ell_{12} & m_{12} & n_{12} \end{bmatrix}\begin{Bmatrix} \bar{U}_1 \\ \bar{V}_1 \\ \bar{W}_1 \\ \bar{U}_2 \\ \bar{V}_2 \\ \bar{W}_2 \end{Bmatrix} \tag{A.38}$$

where ℓ_{12}, m_{12}, n_{12} are given by Eqs. (A.31)

The stiffness matrix of the bar with respect to the global coordinate system is given by

$$\underset{6\times6}{[\bar{k}]} = \underset{6\times2}{[\lambda]^T} \quad \underset{2\times2}{[k]} \quad \underset{2\times6}{[\lambda]} \tag{A.39}$$

A.6 Equivalent Mass Matrix for a Pin-Jointed Bar Element

From Fig. (A.4), the displacements at any point along the length of the bar can be obtained as

$$\begin{Bmatrix} \bar{u}(x) \\ \bar{v}(x) \\ \bar{w}(x) \end{Bmatrix} = \begin{bmatrix} 1-x/\ell & 0 & 0 & x/\ell & 0 & 0 \\ 0 & 1-x/\ell & 0 & 0 & x/\ell & 0 \\ 0 & 0 & 1-x/\ell & 0 & 0 & x/\ell \end{bmatrix} \begin{Bmatrix} \bar{U}_1 \\ \bar{V}_1 \\ \bar{W}_1 \\ \bar{U}_2 \\ \bar{V}_2 \\ \bar{W}_2 \end{Bmatrix} \tag{A.40}$$

or $$\underset{3\times1}{\vec{\bar{u}}} = \underset{3\times6}{[a]} \quad \underset{6\times1}{\vec{\bar{U}}} \tag{A.41}$$

Thus the matrix $[a]$ can be identified as

$$[a(x)] = \begin{bmatrix} 1-x/\ell & 0 & 0 & x/\ell & 0 & 0 \\ 0 & 1-x/\ell & 0 & 0 & x/\ell & 0 \\ 0 & 0 & 1-x/\ell & 0 & 0 & x/\ell \end{bmatrix} \tag{A.42}$$

Assuming the cross-sectional area of the bar A to be constant, the equivalent mass matrix is given by

$$[m]_{6\times 6} = [\bar{m}]_{6\times 6} = \int_{\bar{v}} \rho [a]^T [a] \, d\bar{v} = \frac{\rho A \ell}{6} \begin{bmatrix} 2 & 0 & 0 & 1 & 0 & 0 \\ 0 & 2 & 0 & 0 & 1 & 0 \\ 0 & 0 & 2 & 0 & 0 & 1 \\ 1 & 0 & 0 & 2 & 0 & 0 \\ 0 & 1 & 0 & 0 & 2 & 0 \\ 0 & 0 & 1 & 0 & 0 & 2 \end{bmatrix} \quad \text{(A.43)}$$

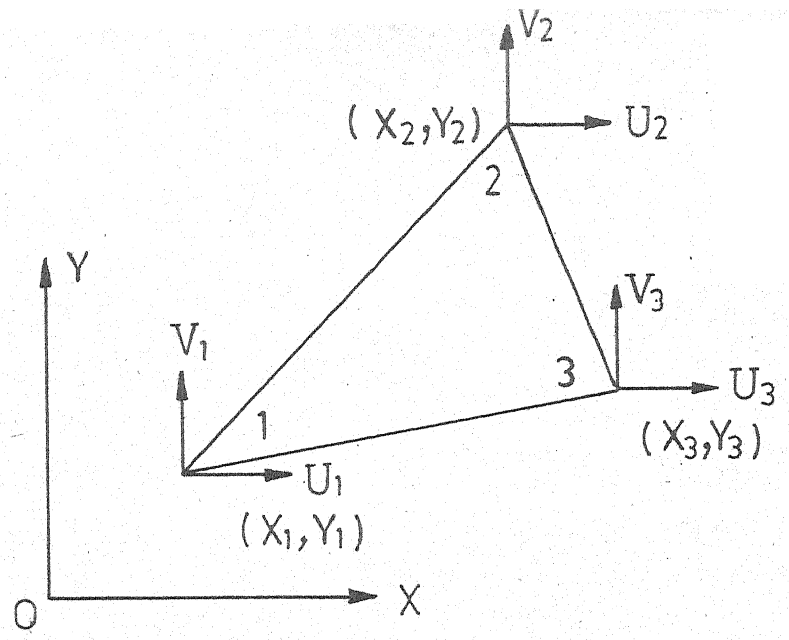

FIG. A.1 A TRIANGULAR PLATE ELEMENT IN LOCAL COORDINATE SYSTEM

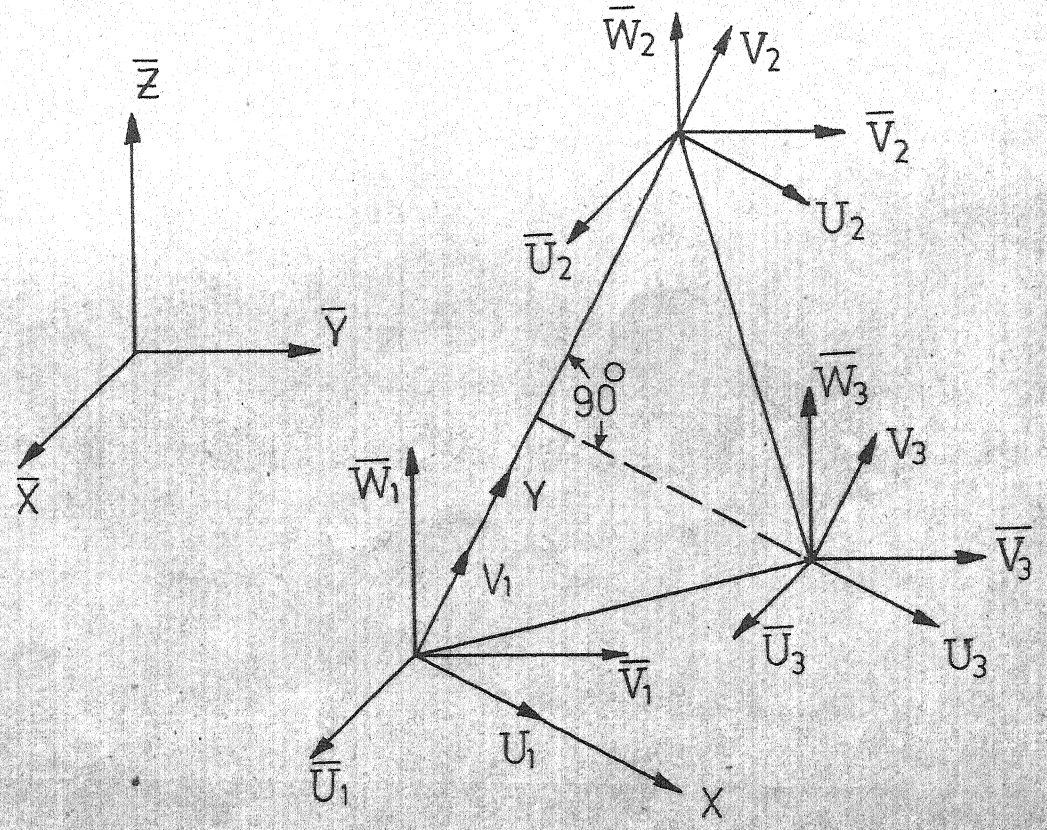

FIG. A.2 A TRIANGULAR PLATE ELEMENT IN GLOBAL COORDINATE SYSTEM

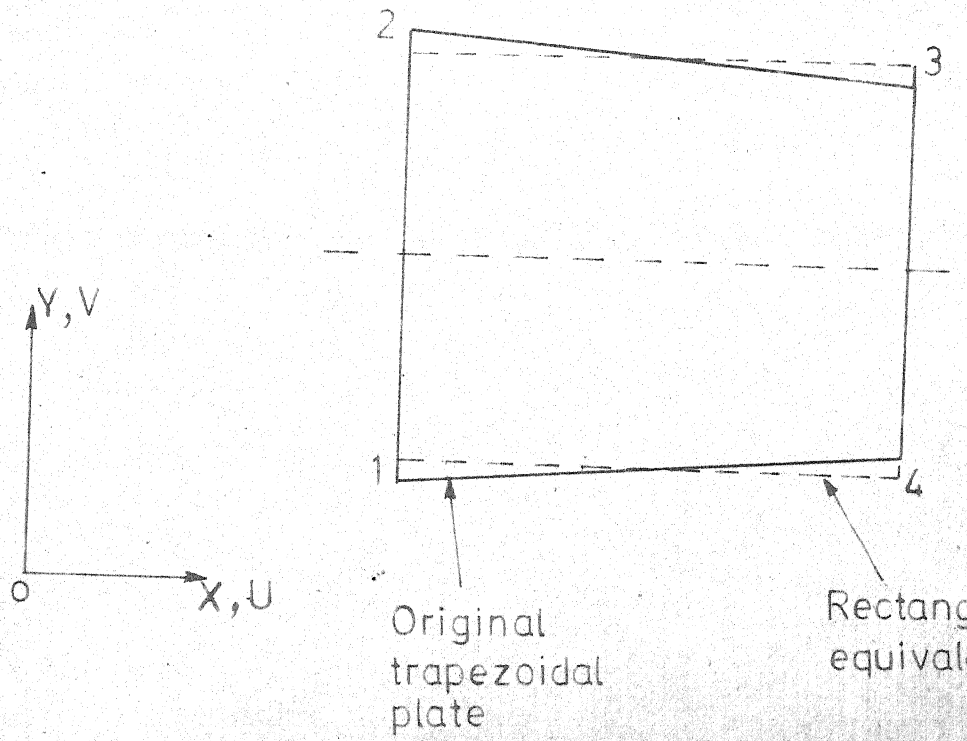

FIG. A.3 TRAPEZOIDAL PLATE APPROXIMATED BY AN EQUIVALENT RECTANGULAR PLATE

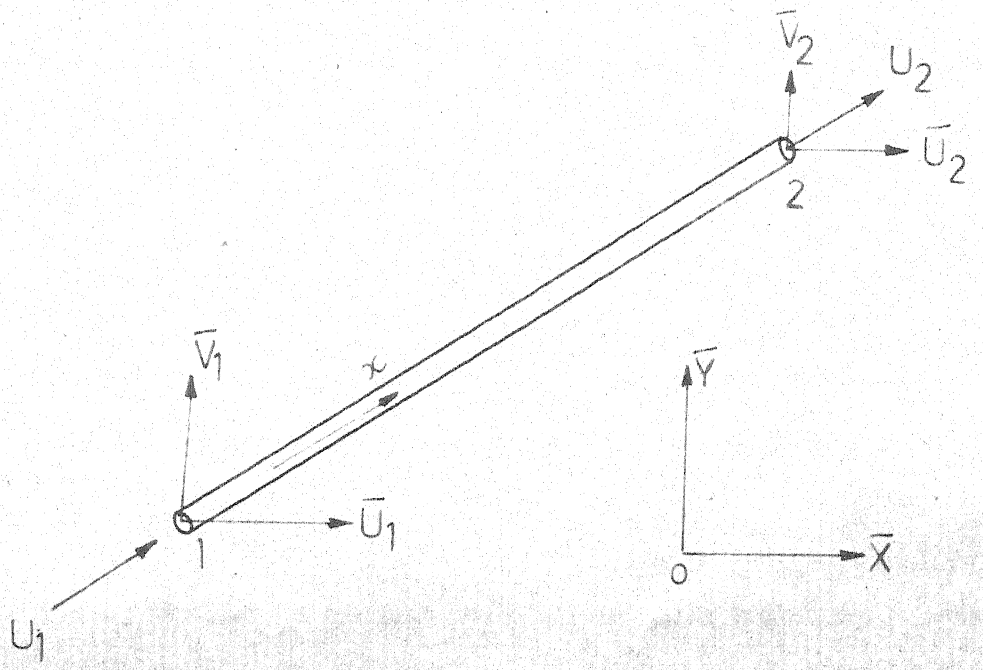

FIG. A.4 PIN-JOINTED BAR IN LOCAL AND GLOBAL COORDINATE SYSTEMS

APPENDIX B

DESCRIPTION OF THE COMPUTER PROGRAMME

The computer programme is written in Fortran IV language for IBM 7044 computer. The programme consists of 18 subroutines which are called by MAIN during optimization stage. This programme can be used to analyze or design any wing structure that could be represented by cover skins, webs and stringers. The programme calculates deflections, stresses, natural frequencies, flutter speeds and flutter frequencies. In design mode the programme can be used to find the minimum weight of wing structure satisfying the strength, stability, frequency, flutter and geometric constraints.

The input data consists of the following information:

(1) Details of the finite element modeling and node numbering scheme.

(2) Material properties of the wing

(3) Details of the payload and flight conditions

(4) A feasible starting design vector

(5) Convergence criteria

The following output can be obtained:

(1) All the input information

(2) An analysis of the wing, if required

(3) The intermediate and final results of analysis and optimization in the design mode.

B.1 Purpose of the subroutines

(1) DFP — It implements Davidon-Fletcher-Powell variable metric method of unconstrained minimization.

(2) FUN — It evaluates the penalty function and its gradient, if the change in design vector is small, using linear approximation, otherwise exact analysis.

(3) FUN1 — Constraints are formulated. Design vector is checked whether it is feasible. The penalty function value is evaluated.

(4) OBJ — It evaluates the weight of wing

(5) XYCORD — It evaluates the dimensions of wing and correlates the design vector to the gauge parameters of the elements

(6) ADATA — It reads all the input information

(7) STORE — It assembles stiffness matrix [SK], mass matrix [SM], aerodynamic matrices [SA], [SB], [SC] and [SD]. Then it performs static analysis, reduces the stiffness and mass matrices using static condensation and obtains the natural frequencies and the associated vectors. Afterwords it calls FLUTER to perform the double eigenvalue analysis

(8) STIF — It determines the type of the element and calls the appropriate subroutine to get elemental stiffness and mass matrices

(9) FLNGE — It gives elemental stiffness and mass matrices for the pin-jointed bar element. Also using the displacement information, it calculates the stresses in the specified elements.

(10) SHEAR It performs the same functions as 'FLNGE' for triangular membrane elements, besides giving the elemental aerodynamic matrices

(11) RCTNGL It performs the same functions as 'FLNGE' for rectangular shear panels

(12) ACROSB It multiplies two real matrices

(13) ATRNSB It also multiplies two real matrices, however it gives $[A^T] \times [B]$

(14) JORDAN It finds the inverse of a real matrix

(15) EREQ It solves the eigenvalue problem using power method

(16) SOLVE It solves $[K] \vec{Y} = \vec{P}$

(17) FLUTER It implements the double eigenvalue analysis of flutter

(18) COMADY It finds the value of a complex determinant

Some of the main features of these subroutines are presented in the form of flow diagram in the next section. The flow charts for other subroutines which use standard algorithms are not included in this flow diagram.

B.2 Flow Diagram

(1) MAIN

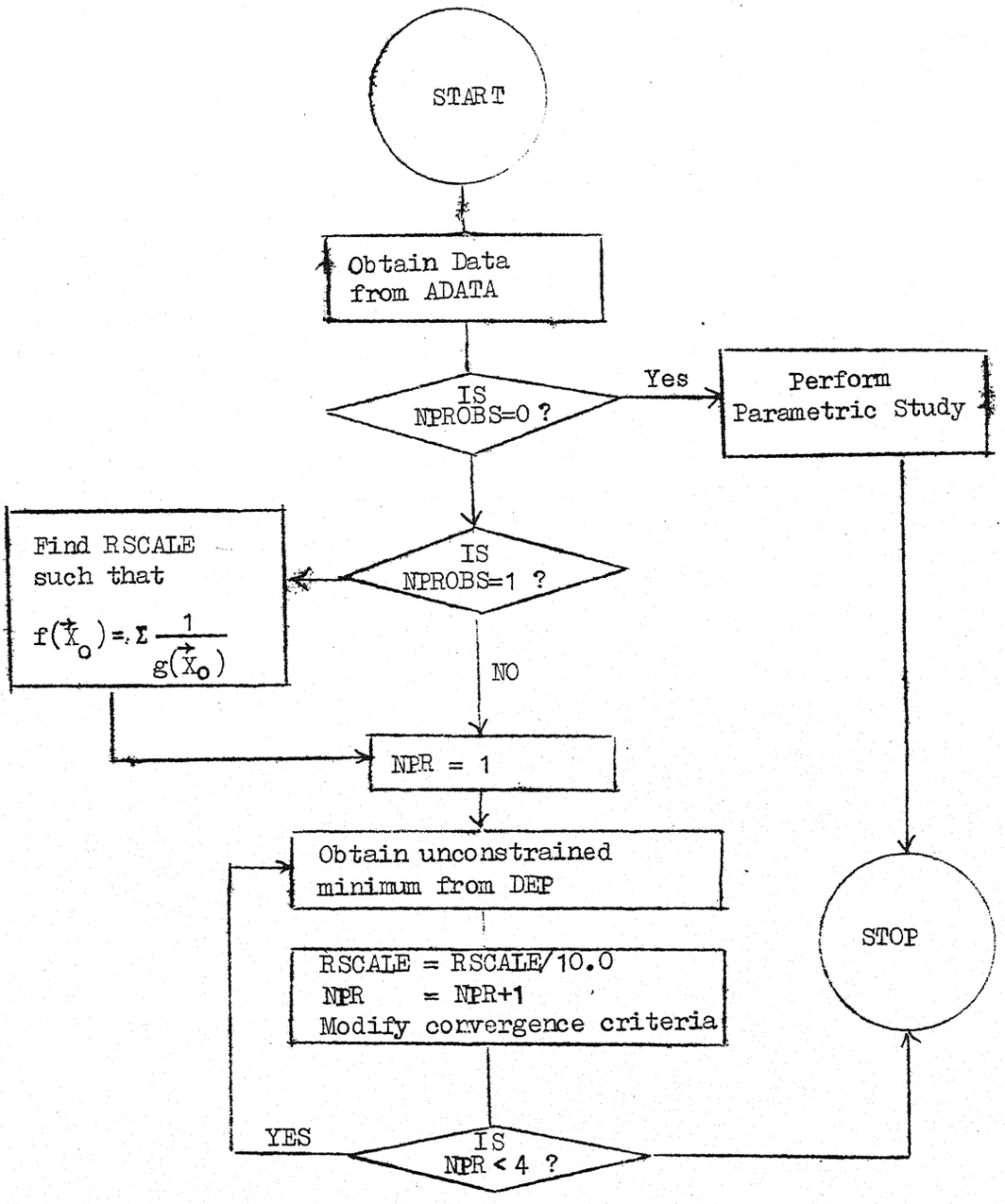

(2) DFP

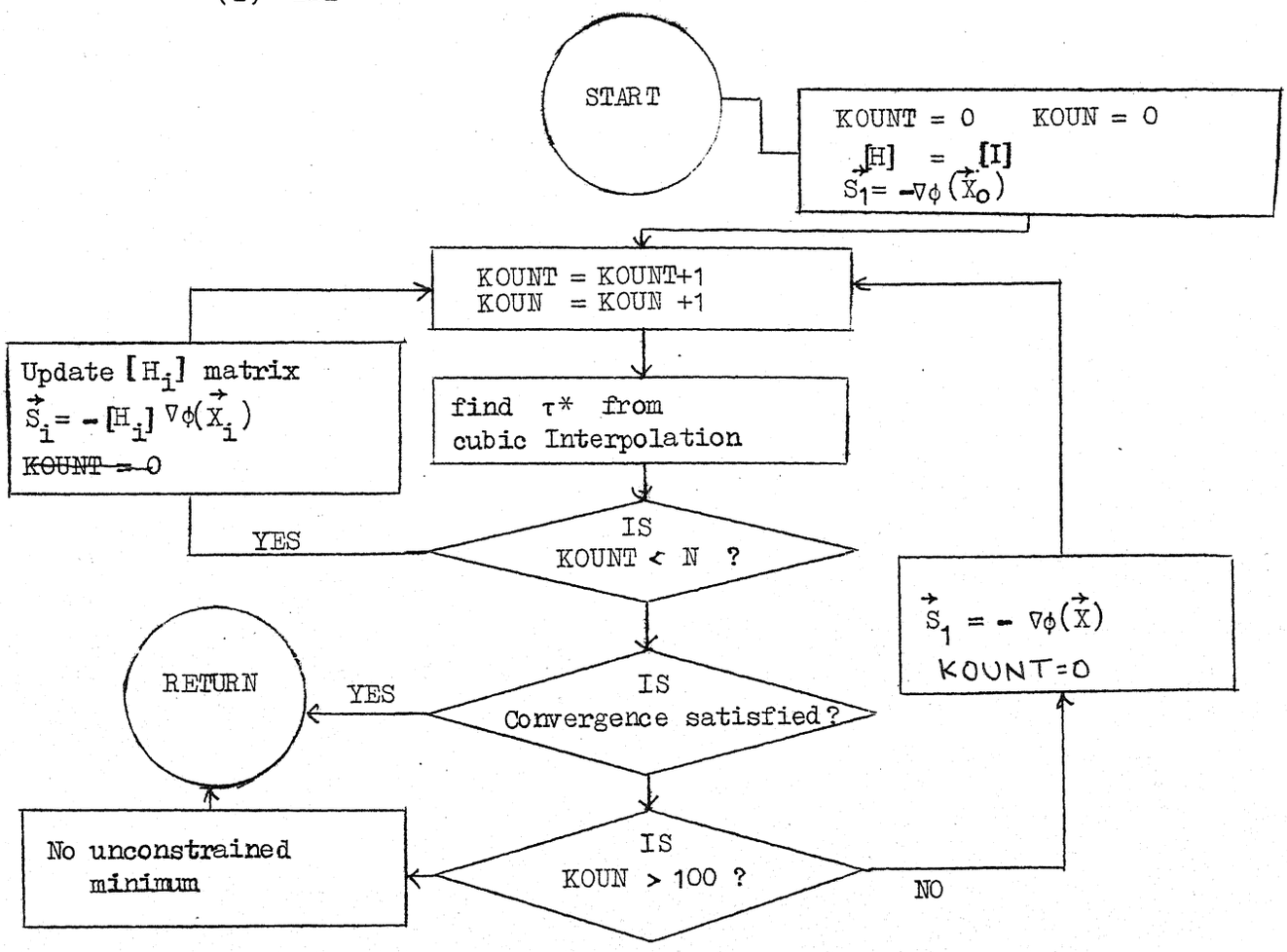
START
KOUNT = 0 KOUN = 0
[H] = [I]
$\vec{S}_1 = -\nabla\phi(\vec{X}_0)$
KOUNT = KOUNT+1
KOUN = KOUN +1
Update $[H_i]$ matrix
$\vec{S}_i = -[H_i]\nabla\phi(\vec{X}_i)$
~~KOUNT = 0~~
find τ^* from
cubic Interpolation
YES
IS
KOUNT < N ?
$\vec{S}_1 = -\nabla\phi(\vec{X})$
KOUNT=0
RETURN
YES
IS
Convergence satisfied?
No unconstrained
minimum
IS
KOUN > 100 ?
NO

(3) FUN

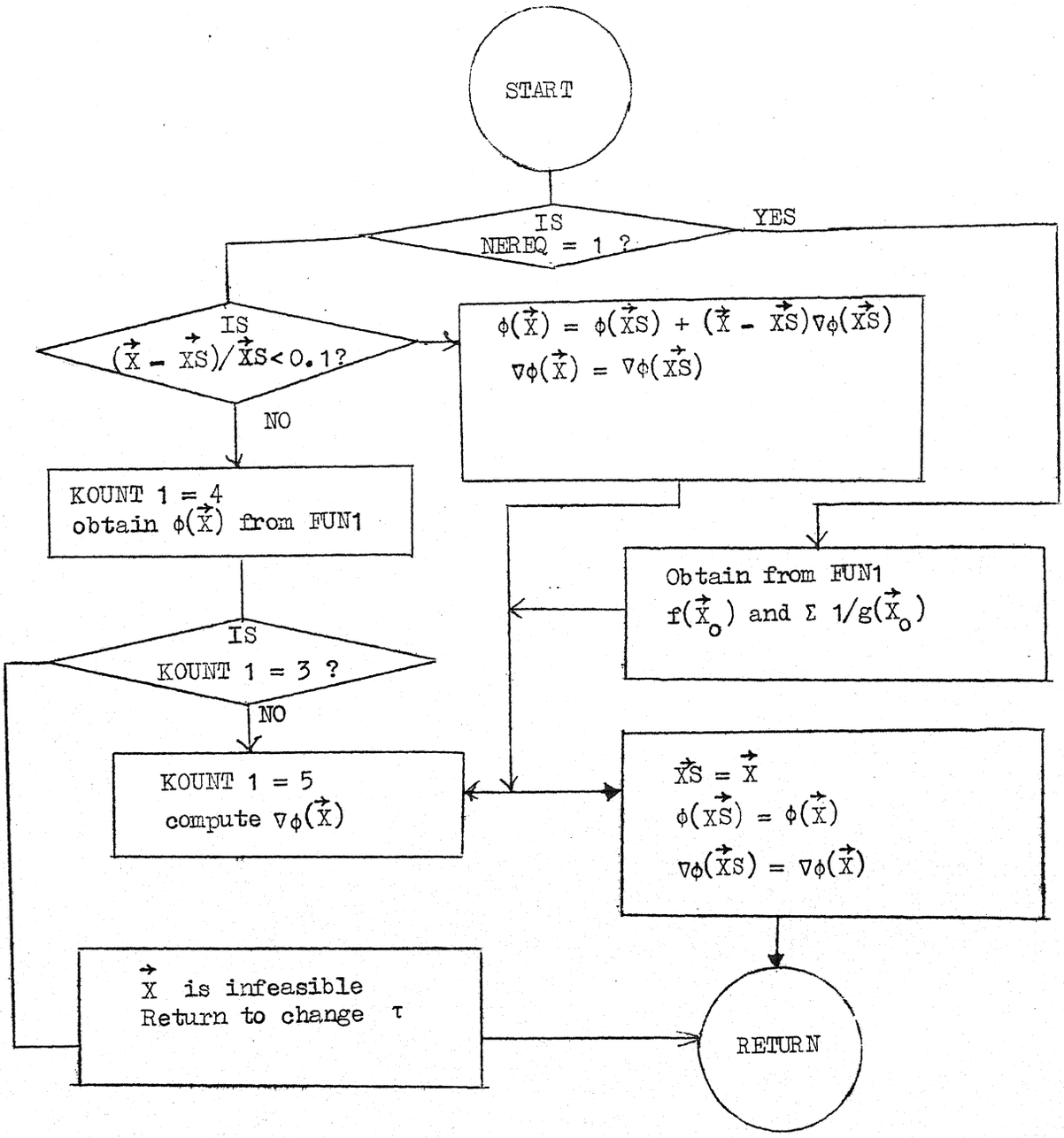
START
IS NEREQ = 1 ?
YES
IS $(\vec{X} - \vec{XS})/\vec{XS} < 0.1$?
NO
$\phi(\vec{X}) = \phi(\vec{XS}) + (\vec{X} - \vec{XS})\nabla\phi(\vec{XS})$
$\nabla\phi(\vec{X}) = \nabla\phi(\vec{XS})$
KOUNT 1 = 4
obtain $\phi(\vec{X})$ from FUN1
Obtain from FUN1
$f(\vec{X}_o)$ and Σ $1/g(\vec{X}_o)$
IS KOUNT 1 = 3 ?
NO
KOUNT 1 = 5
compute $\nabla\phi(\vec{X})$
$\vec{XS} = \vec{X}$
$\phi(\vec{XS}) = \phi(\vec{X})$
$\nabla\phi(\vec{XS}) = \nabla\phi(\vec{X})$
$\vec{X}$ is infeasible
Return to change τ
RETURN

(4) FUN 1

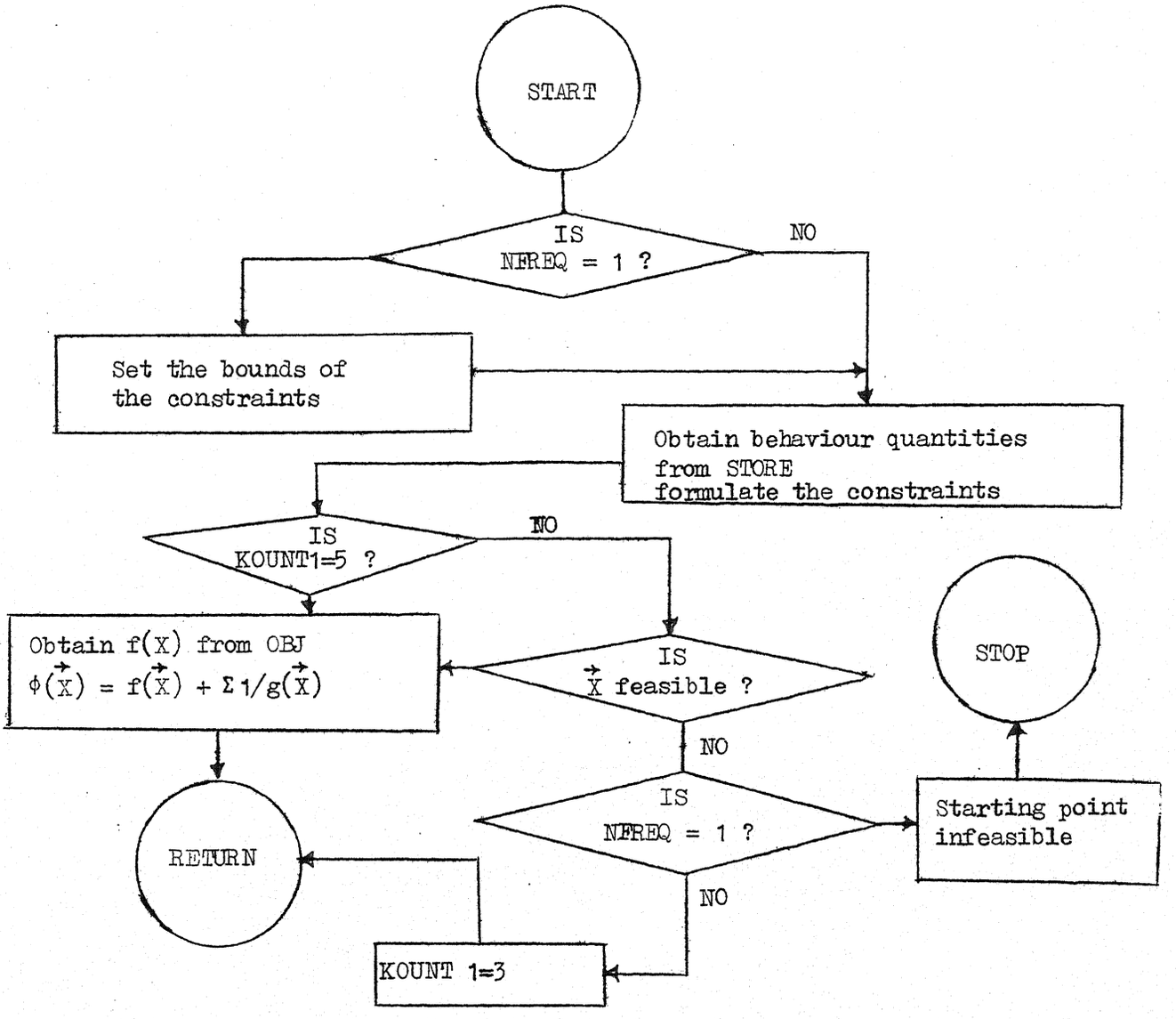
START
IS NFREQ = 1 ?
NO
Set the bounds of the constraints
Obtain behaviour quantities from STORE formulate the constraints
IS KOUNT1=5 ?
NO
Obtain f(X) from OBJ
$\phi(\vec{X}) = f(\vec{X}) + \Sigma 1/g(\vec{X})$
IS $\vec{X}$ feasible ?
STOP
NO
IS NFREQ = 1 ?
Starting point infeasible
RETURN
NO
KOUNT 1=3

(5) STORE

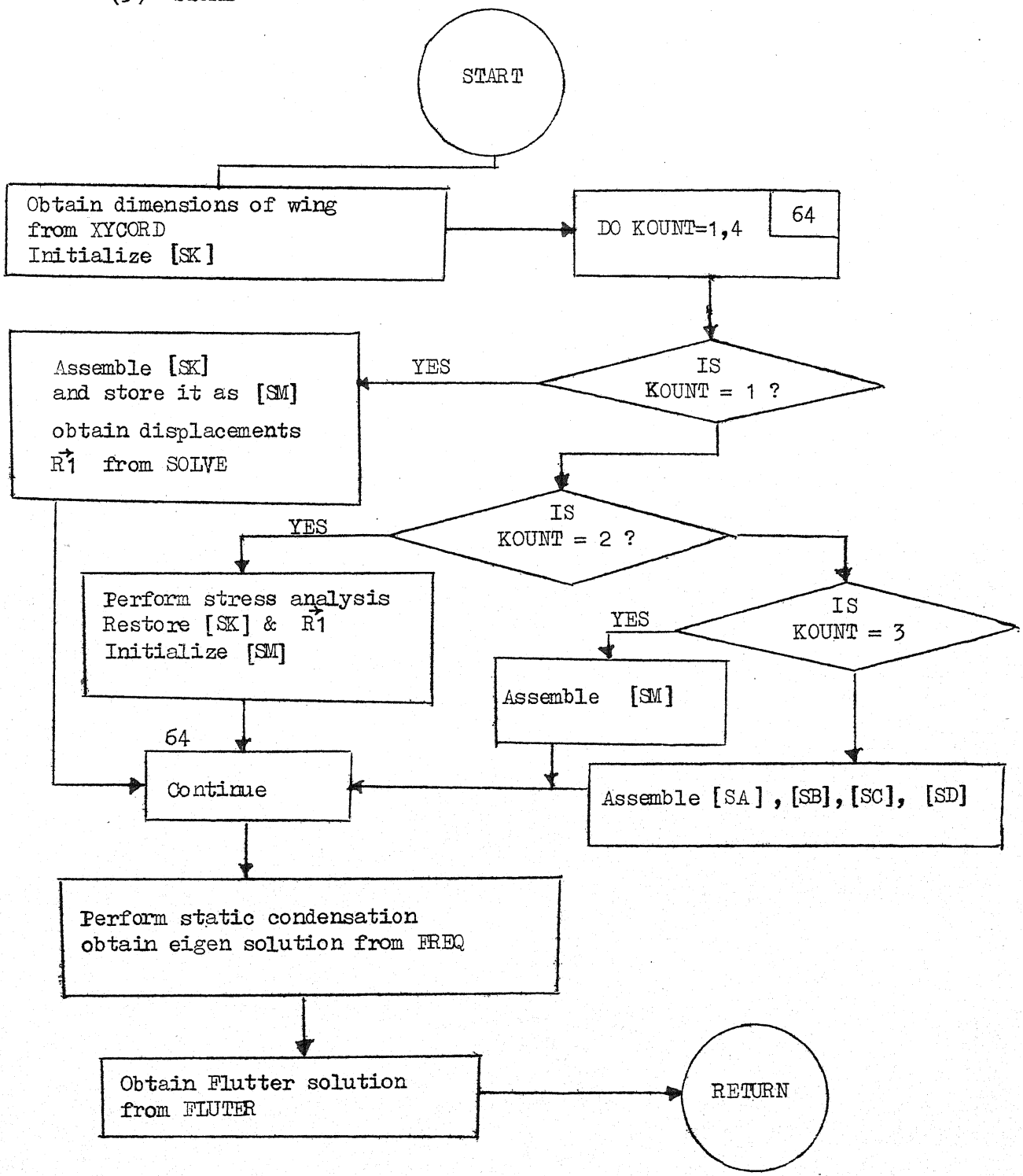
START
Obtain dimensions of wing
from XYCORD
Initialize [SK]
DO KOUNT=1,4
64
IS
KOUNT = 1 ?
YES
Assemble [SK]
and store it as [SM]
obtain displacements
R1 from SOLVE
IS
KOUNT = 2 ?
YES
Perform stress analysis
Restore [SK] & R1
Initialize [SM]
IS
KOUNT = 3
YES
Assemble [SM]
64
Continue
Assemble [SA], [SB], [SC], [SD]
Perform static condensation
obtain eigen solution from FREQ
Obtain Flutter solution
from FLUTER
RETURN

A 91881

AE-1985-M-KIR-AN